applied sciences

MDPI

Review

Review on Mechanisms and Kinetics for Supercritical Water Oxidation Processes

Zhuohang Jiang †, Yanhui Li †, Shuzhong Wang *, Chengchao Cui, Chuang Yang and Jianna Li

Key Laboratory of Thermo-Fluid Science and Engineering of Ministry of Education, School of Energy and Power Engineering, Xi'an Jiaotong University, 28 Xianning West Road, Xi'an 710049, China; jiangzh@stu.xjtu.edu.cn (Z.J.); yhli19@mail.xjtu.edu.cn (Y.L.); ccc3118103069@stu.xjtu.edu.cn (C.C.); cyoung132@stu.xjtu.edu.cn (C.Y.); ljn329@stu.xjtu.edu.cn (J.L.)

* Correspondence: szwang@xjtu.edu.cn

† These authors contributed equally to this work.

Received: 4 June 2020; Accepted: 5 July 2020; Published: 17 July 2020

Abstract: Supercritical water oxidation (SCWO) is a promising wastewater treatment technology owing to its various advantages such as rapid reactions and non-polluting products. However, problems like corrosion and salt decomposition set obstacles to its commercialization. To address these problems, researchers have been developing the optimal reactor design and strengthening measures based on sufficient understandings of the degradation kinetics. The essence of the SCWO process and the roles of oxygen and hydrogen peroxide are summarized in this work. Then, the research status and progress of empirical models, semi-empirical models, and detailed chemical kinetic models (DCKMs) are systematically reviewed. Additionally, this paper is the first to summarize the research progress of quantum chemistry and molecular dynamics simulation. The challenge and further development of kinetics models for the optimization of reactors and the directional transformation of pollutants are pointed out.

Keywords: supercritical water oxidation; wastewater treatment; kinetics model; computational chemistry

1. Introduction

Supercritical water oxidation (SCWO), first proposed by American scholar Modell in the 1980s [1], refers to the process, in which organics are completely decomposed into H_2O and CO_2 as the homogeneous oxidation of organic matters and oxidants (usually excess oxidant) rapidly take place in supercritical water (SCW), water that is in a special state, where its temperature and pressure exceed critical points (374.15 °C, 22.1 MPa), its density is close to that of liquid, and its viscosity, which is about 1–10% of the corresponding liquid is close to that of gas. In general, ordinary liquid water has good solubility for electrolytes, such as inorganic salts, but has no or low solubility for most organic matters and gases, such as CO_2, O_2, N_2, etc. As a result, many organic substances do not react or incompletely react in ordinary water. However, in the supercritical state, the physical and chemical properties of water, such as the ion product constant, density, dielectric constant, and viscosity, have undergone tremendous changes. Due to its lower dielectric constant, SCW makes a better solvent, which can mix with organics and oxygen into a homogeneous phase in any proportion and remain a terribly low dissociation constant and solubility of inorganic salts. Meanwhile, because of its lower viscosity and higher diffusion coefficient, the reactions in SCW are featured by higher reaction speed and better heat transfer capability. Savage [2] pointed out that, compared with other organic solvents, subcritical/supercritical water is conducive to the realization of green, environment-friendly chemical

processes, and has been widely studied in the fields of synthetic fuel production, biomass processing, waste treatment, and material synthesis.

Compared with Advanced Oxidation Processes (AOPs) [3], such as Fenton oxidation [4], electrochemical oxidation [5], and wet oxidation [6], the SCWO technology has following advantages: (1) no interphase mass and heat transfer resistance in SCW, extremely fast reaction speed, and short residence time (usually no more than 1 min) [7,8]; (2) high degradation efficiency. With a 99% removal rate of organic matters and beyond, organic pollutants can eventually be oxidized into CO_2, H_2O, N_2, and other small harmless molecules, and hetero-atoms, such as sulfur, chlorine, and phosphorus, are converted into corresponding inorganic acids [7,9]; and (3) low energy consumption. While the mass fraction of organic matters in the wastewater exceeds 3–4%, the heat balance of the reaction can be maintained without any outside heat of fuel but only by the released heat during the exothermic reaction process [10]. According to the six sectors included in the US National Key Technologies List, SCWO is one of the most promising waste disposal technologies of the 21st century in the "energy and environment" sector. China's Ministry of Industry and Information Technology also listed SCWO as a key technical direction in the field of water pollution prevention and control in 2017 [11].

The SCWO technology has become a superior technology for treating stubborn pollutants that are difficult to be effectively treated by traditional methods, and a small number of commercial devices have been put into operation [2]. Due to harsh SCWO reaction conditions, however, strong corrosion, high material requirements and salt deposition in operation have become the biggest obstacles to its commercialization. Some studies have explored the corrosion characteristics of ferritic-martensitic steels [12,13], TP347H stainless steel [14], Ni-based alloys, [15–17] and Super304H stainless steel [18] in different SCW circumstances. Furthermore, the developed Point Defect Model SCW_PDM has successfully and directly described the oxidation kinetics of metals in supercritical aqueous systems [19]. Additionally, Li et al. [20] studied the effect of salt deposits on corrosion behavior of Ni-based alloys during the SCWO of high-salinity organic wastewater. Since the salt deposit layer restricted the transport of corrosion products and formed a local acidic environment, the corrosion rate of nickel-based alloys accelerated. Meanwhile, obstacles formed by the salt deposit layer for the oxygen transport suppressed the lateral migration of metallic elements and promoted the longitudinal growth of the oxides, thus further roughing the oxide scales. Yang et al. [21] found that the under-deposit corrosion mechanism of Ni-based alloys was affected by environmental temperature. The dissolution-precipitation mechanism was principal at 400 °C while the solid-growth mechanism was primary at 500 °C. Sufficient understandings of organics' degradation kinetics can determine the optimal reaction conditions, which is conducive to the remission of harsh reaction conditions and the reduction of reaction time, so as to further reduce the requirement and corrosion tendency of materials.

Some scholars have reviewed the reactor concepts, industrial status and research status of different pollutants, as well as problems like corrosion and salt deposition in the SCWO system, and provided some possible solutions [6–8,22–26]. In terms of reaction mechanism and reaction kinetics, Watanabe et al. [27] summarized the chemical reactions of C1 compounds in the near-critical and supercritical water, including carbon dioxide, carbon monoxide, formaldehyde, formic acid, methanol, methane and chlorinated methane. Brunner [22] introduced the experimental studies of model compounds and waste materials. Vogel et al. [28] made a detailed comparative analysis of the kinetic data on methanol and found that the kinetic data were affected by the preheating condition of methanol, the initial oxygen-to-methanol ratio, oxidant type, H_2O_2 decomposition, hot zones at high feed concentrations and wall catalysis. Ortiz and Kruse [29] reviewed the process simulation in supercritical fluids and pointed out that molecular dynamics may be the basis for the process simulation which is still based on empirical or semi-empirical approaches. However, the empirical models, semi-empirical models and DCKMs in the SCWO process have not been systematically compared and analyzed. Additionally, although quantum chemistry and molecular dynamics simulations are important for revealing the nature and microscopic mechanism of SCWO reactions, previous reviews did not mention their progress due to the limited computational power.

This article summarizes the essence of the SCWO process and elucidates the roles of oxygen and hydrogen peroxide. Then, the research status and progress of empirical models, semi-empirical models and DCKMs are discussed. Furthermore, this paper is the first to summarize the research progress of quantum chemistry and molecular dynamics simulation. The combination of accurate kinetic models and process simulations can not only predict the degradation of pollutants, but also provide a reference for commercial amplifiers.

2. Fundamental Processes

There are many kinds of chemical substances in refractory organic pollutants such as chemical wastewater, industrial sludge, and landfill leachate. Affected by many factors in SCWO processes, the degradation of organic pollutants in SCWO is a very complex reaction process. Despite the initial reactant as a single organic substance, many intermediates, whose reaction mechanisms are quite complicated, will be formed in SCWO processes. In terms of the reaction type, in addition to oxidation as the main reaction, hydrolysis, pyrolysis, dehydration, polymerization, isomerization, and catalysis also occur simultaneously. As for the nature of reactions, besides the radical reaction as the main reaction under the supercritical condition, the ion reaction also works. These reactions play different roles and account for different proportions under different conditions. Also, the choice of different oxidants will also change the reaction process, and thus affect the removal rate of organic pollutants.

2.1. Reaction Pathways

In the SCWO process, organics only containing C, H, and O have a relatively simple transformation path, by which they can generate corresponding organic radicals and carboxylic acids, and are eventually converted into CO_2 and H_2O. However, when N, S, Cl, and other complex atoms exist, the intermediate products will change and the transformation path will be quite different. The simplified models developed by Li et al. [30] were improved in this section.

2.1.1. Hydrocarbon

Li et al. [30] regarded acetic acid as a refractory intermediate for hydrocarbons degradation, which occurred in the oxidation of all the alcohols except methanol [31]. In the SCWO of aromatic hydrocarbons, understanding the oxidation chemistry of phenol is pivotal since phenol is a stable species [32–34], which would degrade into various carboxylic acids in the subsequent degradation process. The degradation of carboxylic acids in SCWO proceeded with the sequential oxidation from higher molecular weight to lower molecular weight [35]. The simplified reaction network for hydrocarbon oxidation is shown in Figure 1, where $C_mH_nO_r$ can be considered either as an initial reactant or as an unstable intermediate.

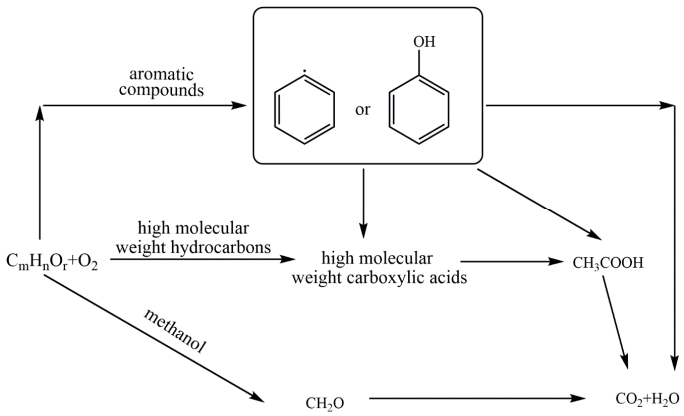

Figure 1. The simplified reaction network for hydrocarbon oxidation in SCW (Adapted from Li et al.'s model [30]).

2.1.2. N-Containing Compound

The degradation of nitrogenous wastes can produce stubborn intermediates, and the resulting acids and/or salts can lead to corrosion and salt deposition in the reactor, so the treatment of nitrogenous wastes in SCWO is relatively difficult [36]. The products of N-containing species include N_2, nitrate, ammonia, nitrite, and NO_x, depending on the state and position of N atoms in organics [37], reaction conditions [38], and the presence or absence of catalysts [39] or auxiliary fuels [40,41]. In the new study, ammonia can be effectively removed through ion exchange with zeolite in intensified SCWO process and ammonia removal was up to 97% when ion exchange was applied to SCWO as a subsequent step [42]. Nitrate is mainly obtained from the compounds containing nitro-group and diazonium, while ammonia is primarily produced from amino-group and N-heterocyclic compounds [37], and N_2 is formed through the interaction of amino and nitro group [43]. Killilea [44] found that all forms of nitrogen, such as ammonia, nitrate, nitrite and organic nitrogen, could be converted into N_2 or N_2O rather than NO_x under appropriate supercritical water conditions, and that N_2O could be further removed by adding catalysts or raising reaction temperature. Additionally, Tan et al. studied the synergistic denitrification mechanism in SCWO processes and found the intermolecular synergistic denitrification between nitro and amino/N-heterocyclic compounds had weaker denitrification efficiency than the intramolecular synergistic denitrification [45]. Figure 2 shows the degradation path of the compound containing N, and $C_mN_oH_nO_r$ can be considered either as an initial reactant or as an unstable intermediate.

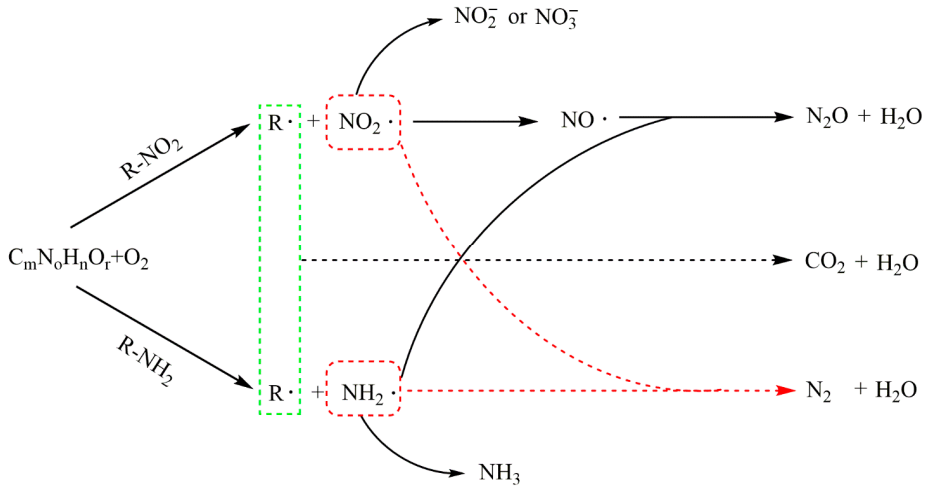

Figure 2. The degradation path of N-containing compounds in SCWO (Adapted from Tan et al.'s model [45]).

2.1.3. Cl-Containing Compound

The Cl-containing compounds degraded in the SCWO process mainly included short-chain chloride and polychlorinated biphenyls (PCBs). The oxidation of short-chain chloride calls for chloroform as the dominant intermediate [30], while the degradation of PCBs had a more complex pathway. Since PCBs are barely soluble in water at normal temperature and pressure, organic solvents such as methanol and benzene are necessary to transport them into the SCWO reactor [46]. Anitescu et al. [47] compared the difference of methanol and benzene as co-solvents on reaction products of 4-chlorobiphenyl in the SCWO process. Methanol could significantly enhance reaction rate compared to benzene. Additionally, relative to the fact that the number of intermediates including toxic dibenzofuran dramatically increased and significant oligomerization occurred when benzene as a co-solvent, methanol as a co-solvent could lead to reaction pathways with less toxic products. The competitive PCB reaction pathways in SCW are shown in Figure 3 [48].

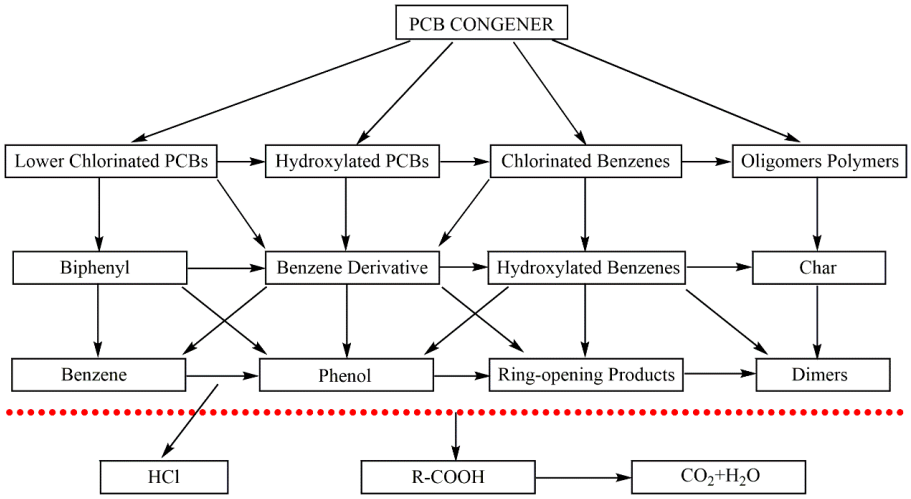

Figure 3. The competitive PCB reaction pathways in SCW [48].

2.2. Ionic Reactions and Free Radical Reactions

The ion product of water, which is related to both density and temperature, increases with temperature rise [49], and is also significantly affected by the density. Relative to the lower ion product of water under the standard state (10^{-14} mol^2/L^2), the ionic product of water reaches the maximum value (>10^{-11} mol^2/L^2) when the pressure is 30 MPa and the temperature is slightly less than 350 °C. This means that the concentration of H^+ and OH^- are more than 10 times larger than that under the standard state and that the acid-base catalyzed reactions such as hydrolysis are promoted. The ion product of water plunges with the decrease of density and the increase of temperature. For example, it is merely ~$10^{-21.6}$ mol^2/L^2 when the water density is ~18 kg/m^3 at 450 °C and 25 MPa. Under this condition, the concentration of hydrogen ion and hydroxide ion is so low, and the free radical reaction is dominant. The special properties of water near the critical point have attracted wide attention. Some scholars have studied the solvation effect of SCW employing quantum chemistry and molecular dynamics simulation. Johnston et al. investigated the effect of solvation on chloride ion and methyl chloride, and found that relative to ambient liquid water, the solvation of ions in SCW increased the reaction rate by 9–12 orders of magnitude [50,51]. Akiya and Savage et al. [52] calculated the dissociation of H_2O_2 in SCW by combining density functional theory (DFT) and molecular simulation (MD). The dissociation activation energy barrier of H_2O_2 in SCW decreased by 2.1 kJ/mol than that in gas-phase due to the solvation.

Moreover, as the water approaches to the critical point, the dissociation constant (K_w) is about three orders of magnitude higher than that in ambient liquid water. The concentration of H^+ produced by the dissociation of water near the critical point is high enough so that some acid-catalyzed organic reactions occur without the addition of any acid. Based on this property, because of hydrolysis as the most typical ionic reaction, many scholars studied the hydrolysis of organics such as indole, phenol and guaiacol under subcritical conditions [53–55]. Biomass resources (such as lignin and microalgae) and wastes (such as sludge and chemical wastewater) were also gasified or partially oxidized under subcritical conditions to produce bio-oil or hydrogen and thus realize clean utilization of biomass and resource utilization of pollutants [56–61]. K_w, however, drops sharply above the critical point. At 600 °C and 250 atm, it is about nine orders of magnitude lower than that in the liquid state [2]. Therefore, the ion reactions are not as significant under supercritical conditions as under subcritical conditions. Tester et al. [62] found that only 2.1% methanol was converted by hydrolysis reaction at 544 °C and 6.6 s residence time, but in the SCWO process above 530 °C, complete conversion (>98%) could be basically achieved. In the presence of alkali metal ions and hydroxide ions, ion dissociation could enhance the ion reaction in SCW and promote the degradation of organic matters. Lee et al. [63]

discovered that the addition of NaOH effectively reduced the formation of dimers and promoted the dechlorination of 2-chlorophenol (2-CP) in the SCWO process of 2-CP and phenol.

In the SCWO process, the oxidants as requisites mainly cause the degradation of organic matters by free radical reactions, which thus tend to play a dominant role rather than ionic reactions. The conversion rate of acetic acid hydrolysis is less than 30%, and acetic acid is completely degraded in the oxidation process at 575 °C, 246 bar and 8 s residence time in the experiment by Meyer et al. [64] Schanzenbächer et al. [65] investigated the hydrolysis and oxidation of ethanol in SCW and found the conversion rate of ethanol during the oxidation was much higher than that during the hydrolysis. The reaction order for oxygen in global rate expression for oxidation was 0.55 ± 0.19, which indicated oxidants played an important role in free radical reactions. Additionally, temperature also greatly affected the formation of free radicals. In the study on the degradation of organic compounds such as methanol [66], ethyl acetate [67] and quinazoline [68], some scholars found that temperature rise effectively shortened the induction time. Henrikson et al. [69] believed that even at the same temperature, different water densities might accelerate or hinder the process of SCW reaction. One possible reason is that in the high water density range, water promotes reactions based on the ion reaction mechanism, while in the low water density range, reactions based on the free radical mechanism are strengthened.

Li et al. [30] proposed the free radical reaction mechanism of SCWO based on wet oxidation and gas-phase oxidation, which included three stages: initiation of chain, development or transfer of chain, and termination of chain.

Initiation of chain:

$$RH + O_2 \longrightarrow R\bullet + HOO\bullet \quad (1)$$

$$RH + HOO\bullet \longrightarrow R\bullet + H_2O_2 \quad (2)$$

$$H_2O_2 \longrightarrow 2OH\bullet \quad (3)$$

Development or transfer of chain:

$$RH + HO\bullet \longrightarrow R\bullet + H_2O \quad (4)$$

$$R\bullet + O_2 \longrightarrow ROO\bullet \quad (5)$$

$$ROO\bullet + RH \longrightarrow ROOH + R\bullet \quad (6)$$

$$ROOH \longrightarrow HO\bullet + RO\bullet \quad (7)$$

Termination of chain:

$$R\bullet + R\bullet \longrightarrow R\text{-}R \quad (8)$$

$$R\bullet + RO\bullet \longrightarrow ROR \quad (9)$$

$$RO\bullet + RO\bullet \longrightarrow ROOR \quad (10)$$

$$R\bullet + ROO\bullet \longrightarrow ROOR \quad (11)$$

Boock and Klein [31] summarized eight key reactions for oxidation in SCW based on a wide range of verified gas-phase and liquid-phase oxidation reactions, which thus constructed a simplified model of the mechanism of Li et al. [30]. Table 1 shows elementary steps and reaction families for oxidation in SCW developed by Boock and Klein [31].

Table 1. Elementary steps and reaction families for oxidation in SCW [31].

Initiation		
1	Hydrogen Abstraction	$RH+O_2 \rightarrow R\bullet+HO_2\bullet$
Propagation		
2	Oxygen Addition	$R\bullet+O_2 \rightarrow RO_2\bullet$
3	H-abstraction	$RO_2\bullet+RH \rightarrow ROOH$
4	Isomerization	$RO_2\bullet \rightarrow HOOR\bullet$
5	β-Scission	$R\bullet \rightarrow R\bullet+C=RH$
Chain Transfer		
6	Disproportionation	$2RO_2\bullet \rightarrow O_2 + 2RO\bullet$
Branching		
7	Decomposition	$ROOH \rightarrow RO\bullet + HO\bullet$
Termination		
8	Radical Recombination	$RO_2\bullet+RO_2\bullet \rightarrow$ Products

Li et al. [30] believed that $HO_2\bullet$ was an important free radical in the reaction process. Reactive oxygen in SCW interacted with the weakest C-H bond to produce the free radical $HO_2\bullet$ and then along with H in organic matters generate H_2O_2, which could also further decompose and thus form hydroxyl radical ($HO\bullet$) that could react with almost any hydrogen-containing compound. When oxygen acted as an oxidant, it first grabbed the hydrogen atoms in the organic material to generate free radicals, which accelerated the subsequent reactions.

Webley and Tester [70] pointed out that the reaction (1) was dominant in the chain initiation stage when developing the DCKM of methane's SCWO. This may be due to the high concentration of methane and oxygen and the low concentration of free radicals at the beginning of the reaction. However, using hydrogen peroxide as an oxidant can directly produce hydroxyl radicals, thus skipping the reactions (1) and (2) in the above chain initiation process. $HO_2\bullet$ is as important as $HO\bullet$ free radical in the SCWO process. Some studies have shown that the concentration of $HO_2\bullet$ is several orders of magnitude higher than that of $HO\bullet$ in the SCWO process [71,72]. Ren et al. explored the key elementary reactions in the thermal combustion process of methanol in SCW through sensitivity analysis. In the chain development stage, the reactions of methanol and corresponding organic radicals with $HO_2\bullet$ and $HO\bullet$ dominated, and the reactions with $HO_2\bullet$ were more critical. Webley and Tester [70] also found that $CH_3+HO_2 \rightarrow CH_3O+OH$ was the most important reaction in the methane SCWO process by a sensitivity analysis.

2.3. Roles of Oxygen and Hydrogen Peroxide

Oxygen and hydrogen peroxide, two most commonly used oxidants in SCWO, have produced very different results when used by different researchers.

Lee et al. [73] compared the effects of hydrogen peroxide and oxygen on oxidation of acetic acid and 2,4-dichlorophenol at 400–500 °C, and the experiments using H_2O_2 as oxidant obtained better degradation results under the same conditions. However, Li et al. [30] claimed that hydrogen peroxide and molecular oxygen had similar oxidation effects. Given this phenomenon, some scholars have studied the oxidation effect and mechanism of oxygen and hydrogen peroxide in the SCWO process.

Since hydrogen peroxide can easily decompose and then produce oxygen and water under heating or light conditions, it is likely to decompose in the preheating stage before the reaction.

Phenix et al. [74] found that when hydrogen peroxide was heated to the supercritical condition, a large amount of oxygen emerged in the product. The total decomposition equation of hydrogen peroxide is shown as follows:

$$H_2O_2 \xrightarrow{k_h} H_2O + {}^1/_2O_2 \quad (12)$$

Tagaki and Ishigure [75] speculated that the above decomposition reaction was carried out through the following paths:

$$H_2O_2 + (M) \xrightarrow{k_1} 2HO\bullet + (M) \quad (13)$$

$$H_2O_2 + HO\bullet \xrightarrow{k_2} H_2O + HO_2\bullet \quad (14)$$

$$HO_2\bullet + HO\bullet \xrightarrow{k_3} H_2O + O_2 \quad (15)$$

$$HO_2\bullet + HO_2\bullet \xrightarrow{k_4} H_2O_2 + O_2 \quad (16)$$

where M in Equation (13) represents the colliding molecules in the reaction, which can be homogeneous substances (such as water) or heterogeneous substances (such as reactor wall) in the reaction system.

As an oxidant with an oxidation capacity only inferior to F_2, OH• free radical with an oxidation potential of 2.8 eV played a key role in the whole oxidation process of organics [30]. An interesting phenomenon emerged by comparing the reaction mechanism between oxygen and hydrogen peroxide. Systems that initially only contained oxygen produced hydrogen peroxide through a propagation reaction, while systems that initially only contained hydrogen peroxide produced oxygen through a thermal decomposition reaction. In the system containing oxygen and water, Tsang W et al. [76] found that the reverse reaction of Equations (14)–(16) existed:

$$H_2O + O_2 \xrightarrow{k_3} HO_2\bullet + HO\bullet \quad (17)$$

$$H_2O + O_2 \xrightarrow{k_3} HO_2\bullet + HO\bullet \quad (18)$$

$$H_2O_2 + O_2 \xrightarrow{k_4} HO_2\bullet + HO_2\bullet \quad (19)$$

Thus, oxygen and water can also generate hydrogen peroxide through the reactions (17)–(19), that is, in the pure SCW environment without organics, no matter whether the initial state of the system is O_2-H_2O or H_2O_2-H_2O, it will be transformed into a mixed system. Under the condition that the transformation is not in equilibrium, the total reaction rate of O_2 and H_2O_2 is different since they have different oxidation rates with organics.

Xiang et al. [77] studied the oxidation of ethanol using a SCWO device with a preheater and obtained the same results when O_2 and H_2O_2 were separately used as oxidants and preheated to supercritical condition. Based on these results, they speculated whether hydrogen peroxide or oxygen was used as an oxidant, they both could be quickly balanced through the above free radical reaction. At equilibrium, the concentration distribution of each species was independent in the initial state, and the subsequent major oxidation process was carried out under such an equilibrium distribution. On the contrary, under the subcritical conditions at 350 °C and 25 MPa, the conversion rate using hydrogen peroxide as oxidant was significantly higher than that of oxygen. This phenomenon may be caused by the mass transfer resistance between oxygen and water and the low decomposition rate of hydrogen peroxide under subcritical conditions.

Lee et al. [73] explored the degradation of acetic acid and 2,4-dichlorophenol using an intermittent SCWO device without preheater. The conversion efficiency of acetic acid when using hydrogen peroxide as oxidant was 8 times higher than that when using oxygen (at 400 °C, a water density of 0.15 g/mL, and a reaction time of 5 min). As the reaction temperature increased, the conversion efficiency difference between the two oxidants decreased. The conversion efficiency ratios of H_2O_2 to O_2 were larger at shorter reaction times, indicating the rapid initial reaction by hydrogen peroxide. However, since hydrogen peroxide can fully mix with the reactants before the start of reaction and oxygen is hard to do so before the supercritical point due to the interphase resistance, it is impossible to determine whether the better oxidation effect of hydrogen peroxide depends on the better oxidation capacity or on the premature reaction before the supercritical point.

Bourhis et al. [78] verified the effect of hydrogen peroxide by a continuous SCWO device. The unheated waste feeds and oxidants were pre-mixed outside the reactor and then mixed with the SCW/air feeds at the reactor inlet to achieve supercritical conditions. The temperature distribution in the reactor was measured by 16 thermocouples, and the degree of reactions was determined by temperature changes at different locations. When O_2 and H_2O_2 were injected together, through analyzing the temperature data curve of isopropanol oxidation, it was found that H_2O_2 mainly played an enhanced role in the initial stage of the reaction, while oxygen mainly played a role in the later stage of the reaction.

The above research indicated that the way oxygen and hydrogen peroxide acted was greatly affected by the heating mode. In a SCWO unit with a preheater, using O_2-H_2O as the oxidant and preheating to supercritical condition had the same effect as using H_2O_2 as the oxidant, and its operating cost was lower. In a SCWO unit without a preheater, using O_2-H_2O_2 as the oxidant may have a faster reaction rate, because there was no mass transfer resistance between H_2O_2 and the organic material, and the reaction may start before the supercritical condition. To enhance the oxidation effect and reduce the operating cost as much as possible, O_2-H_2O in supercritical conditions was used as the main oxidant and mixed with organics and a small amount of H_2O_2 at the reactor entrance. Since the addition of small amounts of H_2O_2 significantly enhanced the initial oxidation rates and O_2 mainly played a role in the later stage of the reaction, the combination of H_2O_2 and O_2 reduced reaction time and operating costs.

In addition to the heating mode of the reaction, the different effects of O_2 and H_2O_2 may also be related to the structural properties of organic compounds. Zhang et al. [79] simulated the reaction process by Chemkin and found the accumulation of HO_2• and HO• in the initial reaction of acetic acid's SCWO. Further, they inferred that the decarboxylation of acetic acid could not be carried out to form HO_2• through the reaction (20), but by the hydrogen extraction reaction by O_2 in the reaction (21), which was consistent with the experimental conclusion of Sean P. Maharrey et al. [80].

$$CH_3COOH + HO\bullet \longrightarrow CH_3COO\bullet + H_2O \quad (20)$$

$$CH_3COOH + O_2 \longrightarrow CH_3COO\bullet + HO_2\bullet \quad (21)$$

Although some scholars have found through macroscopic experiments that the difference between the effect of H_2O_2 and O_2 is due to different effective products at different heating temperatures, the conversion mechanisms of H_2O_2 and O_2 in SCW are still limited. Additionally, since the different effects of O_2 and H_2O_2 may also be related to the structural properties of organic compounds, the microscopic reaction mechanisms of organics with different structural characteristics with O_2 and H_2O_2 remain to be explored.

3. Kinetics Models and Their Development

The study of kinetics is of great significance to reveal the law of migration and transformation of pollutants and meet the needs of reaction process development and reactor design. With the development of research, the reaction kinetics of SCWO has developed from simple models to complex ones, from macroscopic study to microscopic research at molecular and atomic levels. Vadillo et al. [81] have collected the information on main model compounds treated with SCWO.

According to the different modeling methods, the kinetic models of model compounds in the SCWO process can be divided into three categories: empirical model, semi-empirical model and DCKM. The DCKM mainly takes a single substance as the treatment object since it covers a large number of intermediate elementary reaction paths. The data of elementary reaction dynamics are generally derived from quantum chemistry and transition state theory and verified by standardized experiments. When the predicted value is consistent with the experimental result, the reaction mechanism can be explained theoretically, thus guiding the regulation and control ofthe reaction process. For the simultaneous existence of multiple reactants, especially for real pollutants, the studies of

reaction kinetics mainly use empirical models. Since it is difficult to derive accurate reaction rate expressions from elementary reactions and empirical models cannot explain the main reaction processes, the semi-empirical model is derived from a simplified reaction network with measurable changes in intermediate concentration.

3.1. Empirical Model

Empirical models, also known as global kinetics models, usually describe the laws of reaction through power exponential equations, which only involve the concentration changes of reactants rather than intermediates. Kinetics research is very important for the design and operation of the SCWO process. However, since the actual pollutants are usually the mixture of many compounds, it is difficult to identify all the intermediate compounds involved and establish their complex reaction mechanisms. Therefore, the kinetic equations based on COD or TOC removal rate are used to describe the degradation characteristics of complex pollutants and model compounds [82].

Among the current mainstream methods for establishing empirical models, various expressions are different in assumptions or calculation methods adopted in the experimental data processing. Additionally, there is a multi-step kinetic equation that divides the SCWO process into several reaction process distributions to establish the kinetic equation, and a response surface method that can optimize the experimental conditions through polynomial fitting.

3.1.1. Linear Regression Methods

Pseudo-first-order rate expressions: Since O_2 and H_2O are excessive in the SCWO system, their reaction orders are often assumed to be 0, thus simplifying the reaction kinetic equations into the pseudo-first-order rate expressions. As the simplest form of the empirical models, the pseudo-first-order kinetic equations have been widely used to describe the degradation of organics and complex pollutants in the SCWO process. Brock et al. established the pseudo-first-order kinetic equation for SCWO of methanol. The model indicated the induction period of methanol SCWO reaction was shortened with the increase of temperature, but the product distribution was almost independent of temperature. Additionally, the type of reactor and the experimental operation process also affected the establishment of the kinetic equation. Both Anitescu's group [83] and David's group [84] established the pseudo-first-order kinetic equation for SCWO of methanol at 400–500 °C and 25 MPa, but the conversion rates from the two equations were an order of magnitude different.

Multiple linear regression expressions: Multiple linear regression expressions considered the effect of oxygen on the COD removal rate. To use the multiple linear regression expression to solve the power exponent equation, the exponential regression was used to get the function relationship of [COD] with the residence time, as shown in the Equation (22):

$$[\mathrm{COD}] = [\mathrm{COD}]_0 e^{-m\tau} \tag{22}$$

David et al. [84] studied the SCWO kinetics of acetic acid, methanol and phenol using multiple linear regressions. Although the oxygen content in the linear regression data was lower or higher than the stoichiometry and the data for pseudo-first-order rate expressions had an oxygen excess of one order of magnitude regarding the stoichiometry of oxidation reaction, the kinetic consistency of the two methods validated that the rates determining steps of oxidation reaction were similar for 0.4–1.4 oxygen coefficient. J.R. Portela et al. [85] compared the kinetics between subcritical and supercritical water oxidation of phenol. An exponential function was necessary to fit the evolution of the normalized phenol concentration ([phenol]/[phenol]$_0$) versus residence time. The phenol order was 0.95 ± 0.41, which was in agreement with the literature, while the oxygen order was −0.03 ± 0.26, which was smaller than those obtained in the literature due to the great oxygen excess present in all experiments.

3.1.2. Multiple Nonlinear Regression Methods

Relative to linear regression methods, multiple nonlinear regression methods can precisely fit the experiment data and describe the impact of experiment factors at the expense of higher computations. For example, Webley et al. [70] used the POWELL algorithm to establish the kinetic model of supercritical water oxidation of methane at 580–652 °C and 245.8 bar, with the kinetic parameters being in the 95% confidence interval. Additionally, since the Runge-Kutta algorithm can reproduce the global characteristics of the experimental data under the small amount of calculation and Response Surface Methodology (RSM) can describe the reciprocal effect of parameters and find the optimal conditions, both of them were widely used in SCWO studies.

Runge-Kutta algorithm expressions: David et al. [84] compared the kinetic results of multiple linear regression expressions and Runge-Kutta algorithm expressions, thus validating that the Runge-Kutta algorithm was a more efficient method to get real waste kinetic parameters for the scale-up SCWO unit. The oxygen order in the kinetic equations must be considered for better simulation of commercial SCWO devices, thus further optimizing the oxygen consumption and minimizing the operating costs. Sánchez-Oneto et al. [86] established a kinetic model for oxygen concentration dependence in the supercritical water oxidation of cutting fluid wastewater. The oxygen order was 0.58 in the kinetic equation fitted by the Runge-Kutta algorithm, indicating the oxygen concentration had a significant effect on the degradation of cutting fluid wastewater and should be taken into account when establishing kinetic models. Their kinetic model was then used for simulating large scale SCWO processes to evaluate the feasibility of energy recovery in commercial SCWO devices [87]. Additionally, J. Abelleira et al. [88] studied the SCWO kinetics of IPA through the Runge-Kutta algorithm and found that the oxygen order in the kinetic model was 0.774. With high oxygen content, the kinetic model obtained better prediction results at the initial rapid reaction than at the end of the reaction.

Response Surface Methodology (RSM): RSM, a method to find the optimal experimental conditions, explores the relations between several explanatory variables and one or more response variables through multiple quadratic regressions. Different from the above empirical model methods that the kinetic models were obtained by establishing and solving power-law equations, RSM obtained the quantitative relations between the objective function and the process variables through polynomial fitting. Various studies on supercritical water oxidation showed that the oxidation reaction rate was sensitive to many process variables, such as temperature, oxidation coefficient, reaction time, reactant concentration and initial pH value of solution [89–91]. It is necessary to optimize the process variables to obtain optimal conditions since parameters significantly affect the oxidation efficiency. The parameters, however, interact with each other, and the single-factor experiments (i.e., changing one factor while keeping the others constant) that have been used in many studies are insufficient for accurate process optimization [92–94]. In this case, RSM can be used to evaluate the correlation degree of parameters and obtain the optimal conditions, which can effectively reduce the number of experiments, thus saving experiment time and consumptions.

Gong et al. [95] investigated the partial oxidation of landfill leachate in SCW at 450–550 °C, 23–27 MPa, 300–900 s and OC (oxidation coefficient) = 0.1–0.4, and then established the quadratic polynomial models with TOC removal rate (TRE), H_2 yield (GY_{H2}), and carbon recovery rate (CR) as response values to evaluate the effect of the parameters on these values and predict experimental results. With the maximum H_2 yield and the minimum yield of tar and char as constraints, the optimal operating parameters were 550 °C, 24.99 MPa, 851.28 s, and OC = 0.31. Wang et al. [96] applied RSM combined with central composite design and regression analysis to optimize the operating parameters for the oxidation process of Lurgi coal-gasification wastewater in SCW. With TOC and NH3-N degradation rate as response variables and temperature, OR, pressure and residence time as explanatory variables, a regression model was then established, which showed the order for the effect degree of the parameters on the TOC and the NH_3-N degradation rate: temperature > oxygen ratio > reaction time > pressure. Zhang et al. [97] studied the supercritical water oxidation of CI Reactive Orange 7 dye wastewater

using RSM. The results showed that the influence of temperature, oxidant coefficient and reaction time was relatively sensitive in comparison with the pH value.

3.1.3. Multi-Step Rate Expressions

Multi-step rate expressions: Multi-step rate expressions divide the experimental data into several different reaction stages to better describe the SCWO phenomenon. There are various mathematical methods to establish multi-step rate expressions, such as multiple linear regression and multiple nonlinear regression. The common two-step kinetic model divides the SCWO process into the following two stages [88]: (1) a rapid initial reaction, in which reactive molecules are decomposed at a high rate to CO_2, H_2O and a mixture of intermediates of a more refractory nature; (2) a slow subsequent reaction, in which the refractory compounds are gradually decomposed to more simple molecules (alcohols, organic acid, etc.) and eventually mineralized down to CO_2, H_2O, N_2, and salts. Employing tubular reactors and using TOC and COD as the evaluation indices, Abelleira et al. [88] proposed and developed two two-step first-order kinetic models to describe the SCWO kinetics of IPA under oxygen-rich conditions, and these two models had good predictions under oxygen-rich conditions. Xu et al. [98] investigated the catalytic effect of Cr^{3+}/ash for the degradation of naphthalene (Nap) in SCWO and established three-step kinetic equations and two-step kinetic equations for reaction systems with or without a catalyst. For System A (Nap+O_2+H_2O) without a catalyst, the oxidation of Nap was divided into three stages—a fast–slow–fast process: the fast stage, in which H_2O_2 decomposed into H_2O and O_2, the slow stage, in which oxidation occurred in saturated/subcritical water between 200 °C–120 atm and 360 °C–225 atm, and the final fast stage, in which rapid oxidation occurred in near-critical/supercritical water above 360 °C. For the System B (Nap+O_2+$Cr(NO_3)_3$ + $Al_2Si_2O_5{\cdot}(OH)_4$+H_2O), since the catalysis of Cr^{3+}/ash and the oxidation of naphthalene in Stage 2 were faster in System B than in System A, the oxidation process in System B was divided into two stages. The kinetic equations of the two systems are shown in Equations (23)–(25) and Equations (26) and (27), respectively.

Stage 1 of Nap-A

$$-\frac{d[\mathrm{COD}]}{d\tau} = -1.59\times10^{2}\exp\left(-\frac{28.76}{RT}\right)(1-[\mathrm{COD}])[\mathrm{O_2}] \tag{23}$$

Stage 2 of Nap-A

$$-\frac{d[\mathrm{COD}]}{d\tau} = -4.52\times10^{-4}\exp\left(\frac{6.52}{RT}\right)(1-[\mathrm{COD}])[\mathrm{O_2}] \tag{24}$$

Stage 3 of Nap-A(SCWO)

$$-\frac{d[\mathrm{COD}]}{d\tau} = -1\times10^{8}\exp\left(-\frac{139.5}{RT}\right)(1-[\mathrm{COD}])[\mathrm{NT}]^{-0.86}[\mathrm{O_2}]^{1}[\mathrm{H_2O}]^{0.99} \tag{25}$$

Stage 1 of Nap-B

$$-\frac{d[\mathrm{COD}]}{d\tau} = -1\times10^{-2}\exp\left(-\frac{8.72}{RT}\right)(1-[\mathrm{COD}])^{0.22}[\mathrm{NT}]^{-0.78}[\mathrm{O_2}]^{0.2} \tag{26}$$

Stage 2 of Nap-B

$$-\frac{d[\mathrm{COD}]}{d\tau} = -7.27\times10^{-1}\exp\left(-\frac{17.11}{RT}\right)(1-[\mathrm{COD}])^{0.76}[\mathrm{NT}]_0^{-0.24}[\mathrm{O_2}]^{1.8}[\mathrm{H_2O}] \tag{27}$$

The empirical models only reflected the overall trends of the experimental data due to the absence of the complex oxidation process in detail. When different algorithms were used to fit the experimental data, the results would also change accordingly. Table 2 compares the modeling approaches, advantages, and drawbacks of the above algorithms.

Table 2. Comparison of different methods.

Methods	Solving Approaches	Advantages and Drawbacks
Pseudo-first-order rate expressions	(1) With excessive oxygen and the water content more than 90%, the orders of oxygen and water can be assumed as 0 and the order of COD as 1. The kinetic equation can be simplified as follows: $r = \frac{-\mathrm{d}[\mathrm{COD}]}{\mathrm{d}t} = k[\mathrm{COD}]^m[\mathrm{O}]^n[\mathrm{H_2O}]^p \overset{\begin{matrix} m=1 \\ n=0 \\ p=0 \end{matrix}}{\rightarrow} r = \frac{-\mathrm{d}[\mathrm{COD}]}{\mathrm{d}t} = k[\mathrm{COD}]$ (2) Integration of the kinetic equation on residence time leads to the following equation: $-\ln\frac{[\mathrm{COD}]}{[\mathrm{COD}]_0} = k{\cdot}t$ (3) At the same temperature, the relationship of residence time and −ln ([COD]/[COD]$_0$) is plotted and its slope is the rate constant. (4) The Arrhenius Equation is expressed in logarithmic form as: $\ln k = \ln A - \frac{E_a}{R}{\cdot}\frac{1}{T}$ (5) The reaction rate constants at different temperatures are plotted to obtain A and Ea	Only in the case of excessive oxygen can the order of oxygen be assumed as 0 and the kinetic model be simplified into the pseudo-first-order kinetic equation. However, for the consideration of economy, corrosion and other factors, the oxygen in SCWO commercial device is generally under the stoichiometric ratio. Moreover, when the oxygen concentration in the reactor decreases significantly, the reduction of reaction rate is not considered in the pseudo-first-order kinetic equation.
Multiple linear regression expressions	(1) The Arrhenius Equation is substituted into the power type kinetic equation and the order of water is assumed as 0 when the water content is more than 90%. The kinetic equation is shown as follows: $\mathrm{rate} = -\frac{d[\mathrm{COD}]}{d\tau} = A\exp\left(-\frac{E_a}{RT}\right)[\mathrm{COD}][\mathrm{O_2}]^b$ (2) In order to use multiple linear regression to solve the above formula, exponential regression is used to obtain the function between [COD] and residence time, as follows: $[\mathrm{COD}] = [\mathrm{COD}]_0 e^{-m\tau}$ where m is a fitting parameter and τ is residence time.	The effect of oxygen concentration on the degradation rate of organic compounds is considered. However, additional large amounts of experimental data need to be collected since the experiments at the same temperature, the same stoichiometric oxygen concentration and different residence times are necessary.

Table 2. *Cont.*

Methods	Solving Approaches	Advantages and Drawbacks
	(3) The derivative of exponential regression is shown as follows: $$-\frac{d[\mathrm{COD}]}{d\tau} = [\mathrm{COD}]_0 e^{-m\tau}$$ (4) After substituting exponential regression into the kinetic equation, we obtain: $$\text{rate} = -\frac{d[\mathrm{COD}]}{d\tau} = A^* \exp\left(-\frac{E_a}{RT}\right)[\mathrm{O_2}]^b$$ (5) At some point, A^* is a constant and $A^* = A[\mathrm{COD}] = A[\mathrm{COD}]_0 \mathrm{e}^{-\mathrm{m}\tau}$. The logarithmic form of the above formula is shown below: $$\ln\left(-\frac{d[\mathrm{COD}]}{d\tau}\right) = \log A^* - \frac{E_a}{RT} + b\log[\mathrm{O_2}]$$ (6) With COD degradation rate and oxygen concentration as experimental data, the characteristic parameters E_a, A and b can be determined by multiple linear regression of the above equation.	
Runge-Kutta algorithm expressions [86]	(1) The oxygen concentration at any time is expressed as a function of the initial oxygen concentration and the final COD concentration. The oxygen concentration in the reactor can be expressed as follows: $$[\mathrm{O_2}] = ([\mathrm{O_2}]_0 - ([\mathrm{COD}]_0 - [\mathrm{COD}]))$$ (2) The global reaction rate can be deduced as: $$\text{rate} = -\frac{d[\mathrm{COD}]}{d\tau} = k[\mathrm{COD}]([\mathrm{O_2}]_0 - ([\mathrm{COD}]_0 - [\mathrm{COD}]))^b$$	The Runge–Kutta algorithm has two main advantages regarding the multi-linear regression method [86]: (1) Fitting together all experimental data obtained at the same temperature (2) Suppressing the experiments with the same amount of oxygen at any residence time, thus reducing the number of experiments.

Table 2. *Cont.*

Methods	Solving Approaches	Advantages and Drawbacks
	(3) Using the Runge–Kutta algorithm to solve the above differential equation. In this algorithm, the integration interval from 0 to the global residence time (τ_N) is divided into N subintervals with $h = \tau_n/N$. $$\left\{\begin{array}{c} k_1 = f(\tau_n, \mathrm{COD}_n) \\ k_2 = f(\tau_n + \frac{h}{2}, \mathrm{COD}_n + h\frac{k_1}{2}) \\ k_3 = f(\tau_n + \frac{h}{2}, \mathrm{COD}_n + h\frac{k_2}{2}) \\ k_4 = f(\tau_n + \frac{h}{2}, \mathrm{COD}_n + hk_3) \\ \mathrm{COD}_{n+1} = \mathrm{COD}_n + \frac{h}{6}(k_1 + 2k_2 + 2k_3 + k_4) \end{array}\right\}$$ $$n = 0, \ldots, N-1$$ where $\tau_n = n$, h, k_1, k_2, k_3, k_4 are the internal parameters defined in the Runge-Kutta algorithm; $[\mathrm{COD}]_n$ and $[\mathrm{COD}]_{n+1}$ are the calculated COD concentrations at τ_n and τ_{n+1}, respectively. (4) k and b values, as the starting values for the first run of the algorithm, are determined by previous literatures. The experiments are performed at one temperature and different residence times to obtain the $[\mathrm{COD}]_n$. (5) Each model compound is subjected to multiple experiments at different temperatures. The calculated values ($[\mathrm{COD}]_n$) are compared to the final experimental COD concentrations ($[\mathrm{COD}]_{\mathrm{exp}}$) and k and b values are adjusted to obtain the optimal fitting between $[\mathrm{COD}]_n$ and $[\mathrm{COD}]_{\mathrm{exp}}$.	
Response Surface Methodology	Based on the experimental data of different process variables, the quantitative relations between different objective functions and process variables are obtained by the polynomial fitting.	The polynomial fitting relation is established based on a large number of experiments, which is fundamentally different from the above approaches. RSM can analyze the rules of each factor on the objective functions and the interactions between the two factors. However, it cannot obtain the kinetic information of reaction activation energy (E_a), pre-index factor (A), reaction rate constant, etc.
Multi-step rate expressions	For actual wastes and refractory organic compounds, the degradation of organics is often divided into several different reaction stages to better describe the SCWO process. For each stage, the kinetic model can be described by various methods, such as the multiple linear regression and multiple nonlinear regression.	The models can better describe the SCWO process.

3.2. Semi-Empirical Model

Compared with empirical models, semi-empirical models focus on the intermediates for SCWO of organic compounds, which better reflect the degradation pathways of organics. Some scholars have developed lumped kinetic models, which can not only reflect the changes of organic removal rate, but also better realize the quantitative description of intermediate products in the process of degradation.

3.2.1. Small Molecular Substances

In the SCWO process, complex organic compounds are decomposed to various small molecular substances, whose transformation into harmless inorganic substances such as CO_2 and N_2 marks the completion of pollutants' degradation. Hence, it is important to study the transformation of small molecules in SCWO for the complete degradation of organic matters.

Helling et al. [99] established a kinetic model for the oxidation of CO in SCW, by which the oxidation of CO was divided into a direct oxidation reaction with O_2 and a water-gas conversion reaction with H_2O. Webley et al. [70] developed a global mechanism for methane oxidation in SCW on the basis of such a kinetic model. Methane was converted to CO and H_2O first, and then CO directly oxidized with O_2 to generate CO_2, or reacted with H_2O to generate CO_2 and H_2 through water-gas conversion. The model well predicted the changes of O_2 and CO_2 concentrations during the reaction, while CO concentration was underestimated and H_2 concentration was overestimated due to the rapid water-gas conversion reaction. By comparing the yield changes of formaldehyde, CO and CO_2 at different methanol conversion rates, Brock et al. [66] considered that formaldehyde was the initial reaction product and then converted to CO and CO_2. The concentration distribution expressions of each compound were obtained by solving the governing differential equation, which well illustrated the basic characteristics of methanol SCWO. The calculated reaction rate constant indicated that formaldehyde was easier to react than methanol, while CO was not as easy to react as methanol.

3.2.2. Benzene and Its Substituents

Although Yong and Matsunura [100,101] deduced the reaction pathway of benzene decomposition in SCWG that benzene formed phenol and gas, directly or through naphthalene as an intermediate medium, into char and other liquid products, and mainly transformed to phenol under the oxygen-rich condition in SCWO. Dinaro et al. [102] found benzene reacted almost exclusively by $C_6H_6+OH \rightarrow C_6H_5OH+H$ and $C_6H_6+OH \rightarrow C_6H_5+H_2O$, with the latter accounting for over 97% of the oxidation rate of benzene at 813 K and 246 bar. The C_6H_5 benzyl radical captured O_2 to form $C_6H_5O_2$ and underwent unimolecular dissociation to form C_6H_5O phenoxy radical and OH• with $C_6H_5O_2H$ as an intermediate in subsequent steps. Due to the stability of phenoxy radical, its quenching reaction led to the formation of phenol at low temperatures [32].

Gopalan and Savage [103] investigated the degradation pathway for phenol oxidation in SCW based on the analysis of the free-radical chemistry of phenol oxidation in both gas and solution phases. The degradation of phenol included two main competing reactions, dimer formation and ring-opening reaction, in which the formation of dimers including 2- and 4-phenoxyphenol, dibenzofuran and 2,2′-biphenol was caused by the reaction between phenoxy radicals. The gas-phase combustion reaction for phenol at above 1000 °C would decay at 710 °C [104], which was inconsistent with the reaction temperature of SCWO. The reaction products of SCWO were also inconsistent with the gas-phase combustion mechanism because the formation of peroxy radicals was reversed under the SCWO condition, indicating a large number of peroxy radicals in the SCWO reaction could not be generated by this mechanism. However, the mechanism of phenol for ring-opening in the liquid phase involved aldehydes and acids as intermediates [105], which may be applied under SCWO conditions since formic, glyoxalic, oxalic, propionic, hydracrylic, succinic, and maleic acids have all been detected in phenol SCWO.

Matsumura et al. [106] analyzed the effect of phenol concentration on reaction intermediates at constant oxygen content. The reaction product distribution varied with concentration and tarry material production was observed in high phenol concentration phenol, which was probably because the concentration of phenol did not affect the initial phenol decomposition reaction but the subsequent radical reaction. The high phenol concentration accelerated the additive reaction between aromatic compounds. Additionally, the reaction pathways for the SCWPO of phenols were also investigated [107]. Guan et al. [107] developed the pathways and a kinetic model of partial oxidation phenol at 450 °C and 24 MPa, which included nine reaction paths and eight kinetic equations. The model precisely depicts the concentration changes of CO, H_2 and CO_2, in which CO concentration initially increased rapidly, peaked, and then dropped slowly, while H_2 and CO_2 concentration increased slowly after a rapid increase in the beginning. Figure 4 depicts the four types of main reactions for partial oxidation phenol, including (1) phenol oxidation (both dimerization and ring-opening), (2) acid oxidation, (3) acid gasification, and (4) gaseous products interconversion. The kinetics model again presented the experimental results well and had good predictions for the composition of the gas effluent. It is worth noting that the rate constant for dimers formation (k_1) was extremely small, indicating phenol barely converted to dimers in the presence of oxygen.

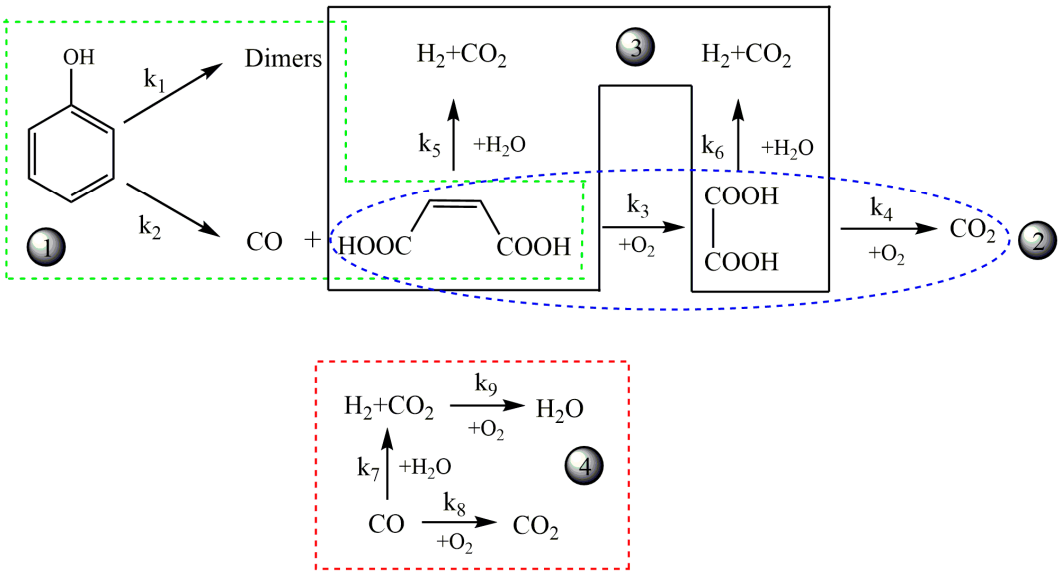

Figure 4. The reaction pathways for partial oxidation of phenol in SCW [107].

Except the oxidation of benzene and phenol, Martino and Savage reported the SCWO of phenols with -CH_3, -CHO, -OH, -OCH_3, -NO_2, -C_2H_5, and –$COCH_3$ substituents [33,34]. The appearance of substituents accelerated the oxidation rate compared with phenol itself and both the identity and location of the substituents affected the oxidation rate of substituted phenol. The reactivity of different isomers was in the order of ortho > para > meta for all of the substituted phenols. Figure 5 shows the reaction network for SCWO of monosubstituted phenols [34].

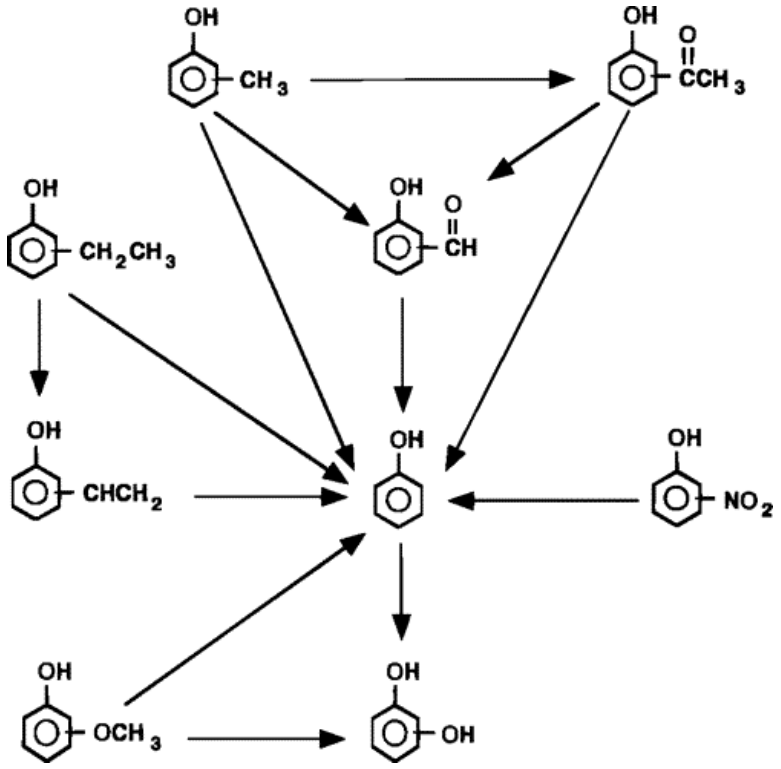

Figure 5. Reaction network for SCWO of monosubstituted phenols [34].

3.2.3. Polycyclic Aromatic Hydrocarbons

Polycyclic aromatic hydrocarbons (PAHs), the largest, ubiquitous and carcinogenic environmental chemical groups, have a wide range of sources like oil extraction, petroleum refining, coal mining, bush fires and coal burning [108]. Some studies have investigated the degradation pathways of biphenyl [108,109], fluorine [108], and naphthalene [98,110] in high-pressure hot water.

Gheorghe et al. [109] developed principal reaction pathways in the biphenyl SCWO reaction network, as shown in Figure 6. In their research, more than 50 intermediates detected under various SCWO conditions were mainly benzene derivatives such as acetophenone and dibenzofuran. The degradation of biphenyl was initiated by OH• to hydroxylbiphenyl, in which *ortho*-hydroxylbiphenyl and *para*-hydroxylbiphenyl are more reactive than *meta*-hydroxylbiphenyl. The hydroxylbiphenyl formed open-ring carbonylic compounds through keto-enol tautomerism in the subsequent oxidation process and eventually into mineral products. However, Onwudili and Williams [108] found different ring-opening products, such as phenylethene, benzaldehyde, phenylethen-2-ol, and acetophenone, when investigating the degradation of biphenyl. This was probably caused by lower temperatures (<380 °C) and pressure (<22.5 MPa) while Gheorghe's study [109] was carried out in higher temperatures (673–823 K) with methanol as the auxiliary fuel.

Xu et al. [110] summarized a four-step oxidation process for naphthalene degradation in SCW: (1) One benzene ring breaks and forms light hydrocarbons such as formic acid, acetic acid and other aromatic hydrocarbons including aromatic carboxylic acid, ketone and aromatic ester. (2) The polymerization of some intermediates forms dibenzofuran, fluorenone and 2′-hydroxyacetophenone. (3) Light hydrocarbons and polymers oxidize and produce acetic acid at the same time during the polymerization. (4) Acetic acid and other intermediates decompose to CO_2 and H_2O. Figure 7 displays the reaction network for naphthalene degradation in their subsequent studies, including five main ways (R01–R05) for oxygen to "invade" naphthalene rings [98].

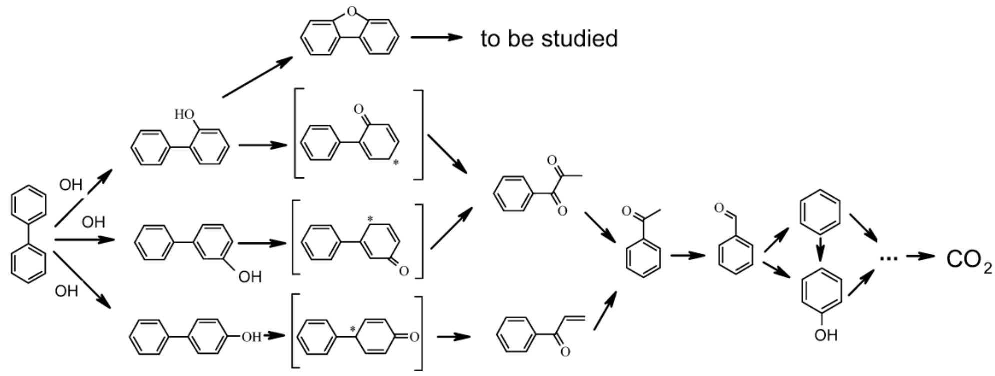

Figure 6. Simplified reaction network for SCWO of monosubstituted phenols [109].

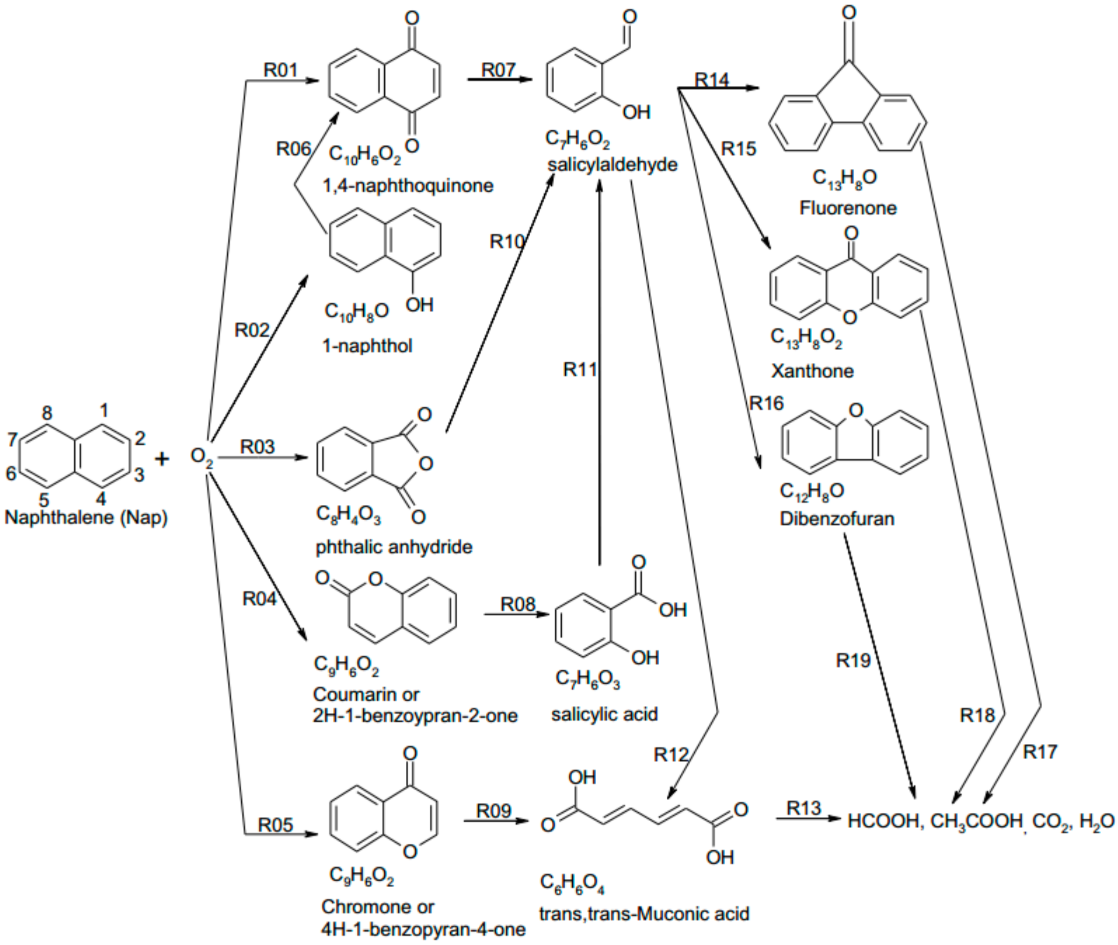

Figure 7. Reaction network for SCWO of naphthalene in batch reactors [98].

As expected, the oxidation of fluorine started with OH• attacking the saturated carbon on the fluorene molecule, which is similar to most other organic compounds [108]. The intermediates found included biphenyl, benzophenone, dibenzofuran, benzofuran, hydroxybenzofuran, xanthone and fluorenone, of which fluorenone is the key intermediate and very stubborn at a lower temperature. The formation of 9-fluorenone, which led to the formation of xanthone or decomposed to benzaldehyde, phenol, acetophenone and other single-ringed aromatic compounds subsequently, may be the major pathway for fluorene oxidation under hydrothermal conditions. Furthermore, the oxidation of fluorene can also be carried out by another possible route, by which the –CH_2O group was removed from hydroxylfluorene and 9-fluorenone decarbonylate, leading to the significant production of biphenyl observed. Hence, after the formation of biphenyl, the process assumed the pattern earlier described for

biphenyl oxidation in their early study [108]. The further decomposition products included benzofuran, isobenzofuranone, acetophenone and benzoic acid, and the detailed mechanism for fluorene oxidation is presented in Figure 8.

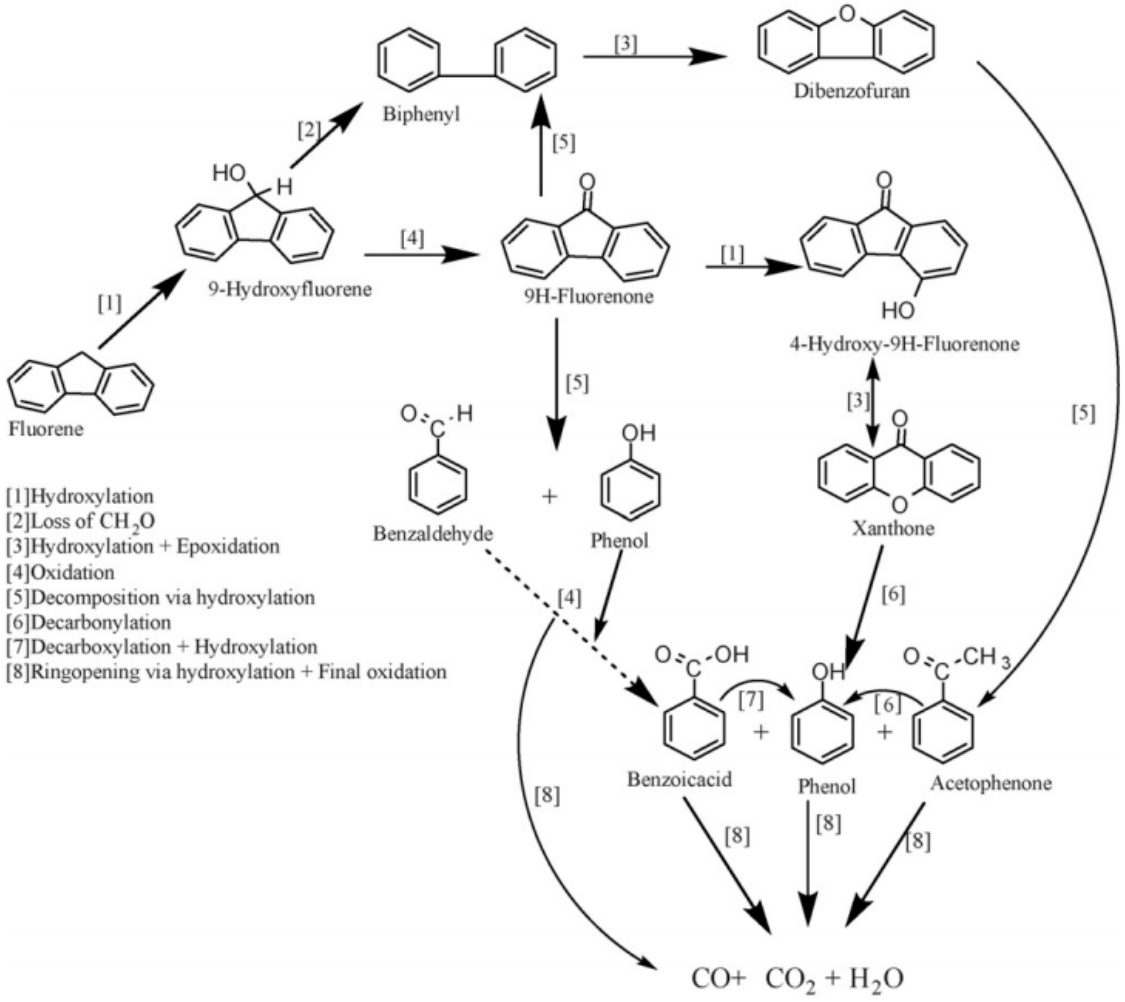

Figure 8. Reaction mechanism for SCWO of fluorine [108].

3.2.4. Heterocyclic Compounds

Crain et al. [111] studied reaction pathways, transition products and the kinetics of pyridine oxidation in SCW, and constructed a simplified reaction network. On the assumption that the initial reaction involved hydrogen abstraction followed by hydroxylation, all ring cleavage reactions were related to the formation of 2-, 3-, or 4-hydroxypyridine and its resonance isomer. The different product distribution in liquid effluent indicated that the reaction sites of hydroxyl substituted pyridine ring-opening and chain fracture after ring-opening were not unique. (i.e., the presence of maleic acid suggested at lease one nitrogen-carbon bond was broken and only the rupture of two carbon-carbon bonds could produce dimethylamine). It suggested a variety of products of 2-, 3-, or 4-hydroxypyridine ring-opening and carbon chain rupture, including glutaconic acid + NH_3, maleic acid + methyl amine, malonic acid + ethyl amine, and dimethyl amine + acetone. The above-mentioned products degraded into different carboxylic acids, alcohol molecules and amino organic compounds, and eventually into inorganic substances such as NH_3, CO_2, and H_2O. Figure 9 summarizes partial simplified reaction pathways of pyridine oxidation in SCW.

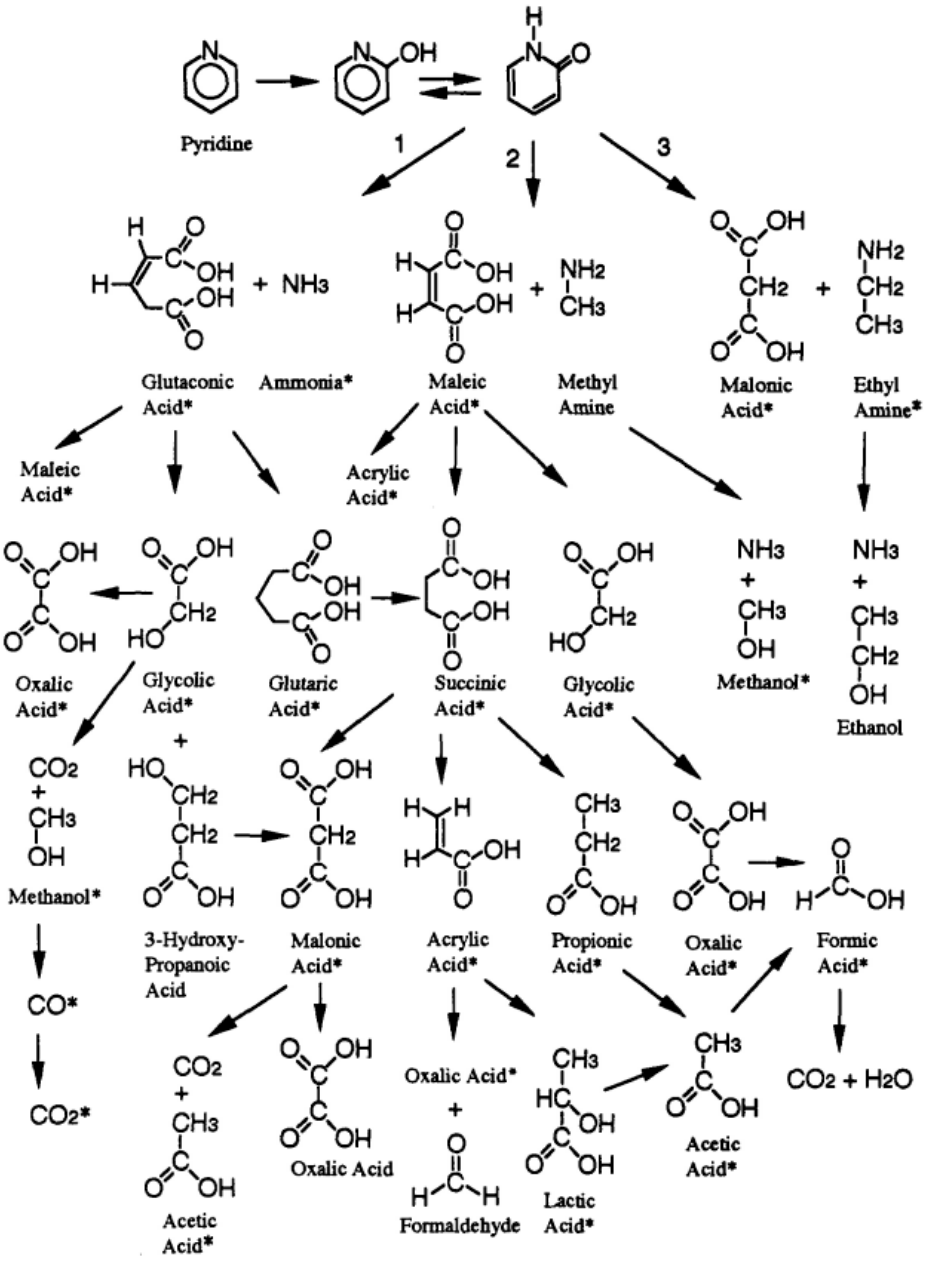

Figure 9. Partial simplified reaction mechanism for pyridine oxidation in SCW (*, compounds identified in their study) [111].

Gong et al. [68,112] investigated the reaction pathways of quinazoline oxidation in SCW, and found the oxidation of quinazoline included two ring-opening reactions: the ring-opening reaction on the benzene ring and the ring-opening reaction on the pyrimidine ring. Since the two N atoms in the pyrimidine ring, whose presence was attributed to the low electron cloud density in the pyrimidine ring [113], had a stronger ability to attract electrons, The benzene ring would be vulnerable to oxidation. The simplified reaction model based on the measured intermediate is shown in Figure 10 [68], and a quantitative kinetic model with 11 reaction pathways involved was proposed to describe the reaction pathways, which well matched most of the experimental concentration changes of major compounds (quinazoline, pyrimidine, naphtalene, phenol, NH_3, CO_2, etc) at test temperatures between 673–873K. However, the model overpredicted NH_3 concentration at 773K and underestimated NH_3 concentration at 873K. The sensitivity analysis determined that the reaction was dominated by the selective ring-opening of quinazoline for pyrimidine yielding. When the temperature was

above 823K, the reaction rate of pyrimidine degradation was significantly accelerated. Additionally, Ren et al. [114] studied the degradation of quinolone in the SCWO process and proved that quinoline had comparable "ignition temperature" as methanol and isopropanol. The ring-opening reaction was a rate-limiting step. The ring-opening reaction on the pyridine ring was more difficult than that on benzene, which was consistent with studies on quinazoline degradation [68,112]. The reaction pathway can be proposed as quinoline → secondary components → volatile species → gaseous products.

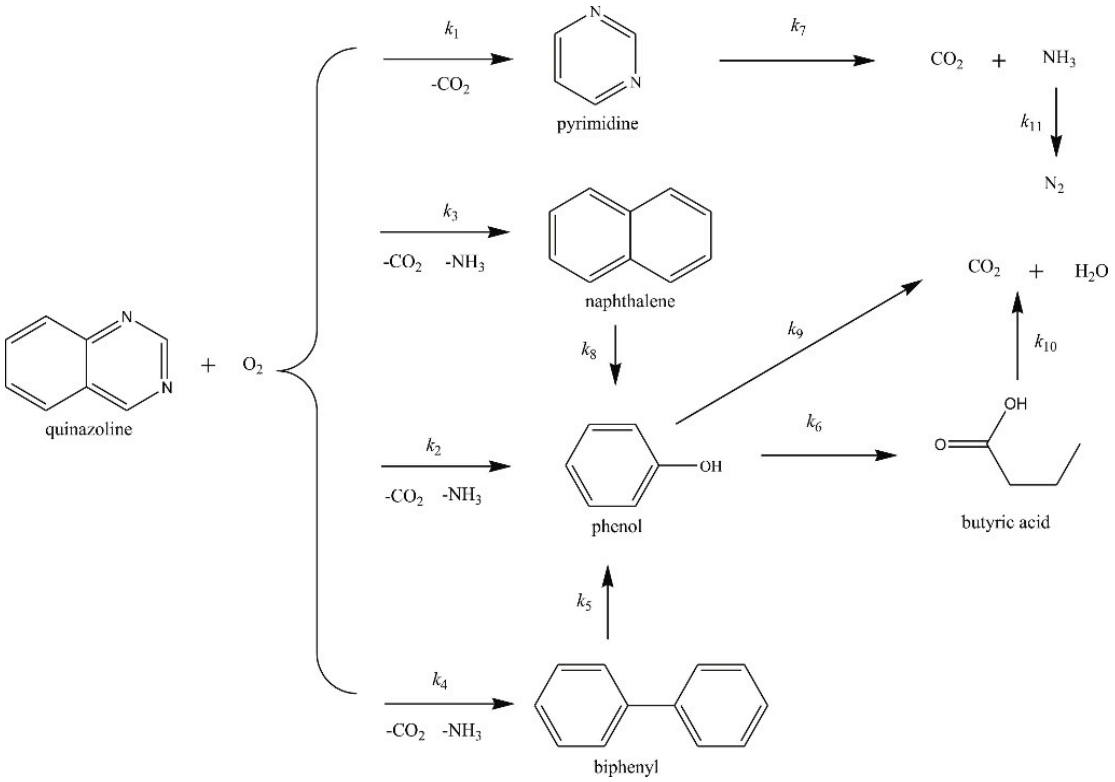

Figure 10. Simplified reaction network of oxidative degradation of quinazoline in SCW [68].

Li and Lu [115] analyzed the migration of N element during the oxidation of quinazoline in SCW using ReaxFF reactive force field combined with the DFT method. A long carbon chain with N atoms was formed by the ring-opening reaction on the pyrimidine ring, and subsequently broke into several small fragments, of which C≡N fragments were vital for the formation of NH_3. C≡N fragments fractured into CO and NH_2 after being attacked by OH•, O_2, and H_2O in turn, and the highly unstable NH_2 extracted H atoms from the SCW to form NH_3. However, the extremely small number of N_2 molecules in the simulation results may be caused by the steric hindrance and the small number of N atoms in the simulation system.

3.3. DCKM

DCKM, which consists of a large number of primitive reactions, provides a detailed quantitative description of the chemical behavior of all molecular components and reaction intermediates. In addition, its composition makes the prediction of reaction situation possible. Compared to empirical models, which are simple in form and can be easily coupled with flow and heat transfer equations for SCWO reactor optimization, complete DCKMs are too complex to be coupled with flow and heat transfer equations to quantitatively describe a reacting flow. Hence, in addition to the development of DCKMs for organics in the SCWO process, it is also important to develop models with simplified mechanisms that are still representative of the chemical reaction process, thus enabling the development of SCWO simulation models with chemical reactions and the further design optimization of SCWO reactors [116].

The high temperature and pressure reaction conditions of the SCWO technology make it difficult to apply some measurement techniques, erecting a barrier to the establishment of DCKM under SCWO conditions. However, the SCWO reaction process is similar to the gas-phase combustion process in some free radical reactions, and gas-phase combustion has developed numerous DCKMs of organics. Currently, some scholars have developed DCKMs of various compounds based on gas-phase combustion [31,66,72,102,116–126]. The goal of this section is not to summarize these studies, but to analyze the development and simplification treatment of DCKMs for hydrogen, methanol, acetic acid, benzene and ammonia. The main bases for the selection of model compounds in this section are as follows: Hydrogen is regarded as a possible auxiliary fuel to heat release for low heat value waste [117,118]. Moreover, the mechanism for hydrogen oxidation will directly be used as a subset for the oxidation mechanisms of other complex substances [119]. As the most common auxiliary fuel in SCWO and hydrothermal combustion processes, methanol has an important role in regulating reaction strengthening and degradation process. Stubborn compounds, such as acetic acid, benzene, and ammonia, are often key products in the degradation of organic matters and have a significant impact on global oxidation kinetics.

3.3.1. Hydrogen

Holgate and Tester [119] developed a DCKM for the SCWO of hydrogen based on a validated gas-phase mechanism and corrected for the high-pressure environment by techniques such as RRKM theory. The major free-radical reaction pathways in DCKM for hydrogen oxidation in SCW are shown in Figure 11. The 19-reaction mechanism in model YDR91J can be approximated by the seven dominating fast reactions (see Table 3), which are several orders of magnitude faster than the others. The model reproduced nearly all of the global characteristics of the experimental data, such as hydrogen conversion, hydrogen concentration and oxygen concentration. Additionally, the fast rate of $H+O_2+M \rightarrow HO_2+M$ may lead to the reaction's global independence of oxygen concentration.

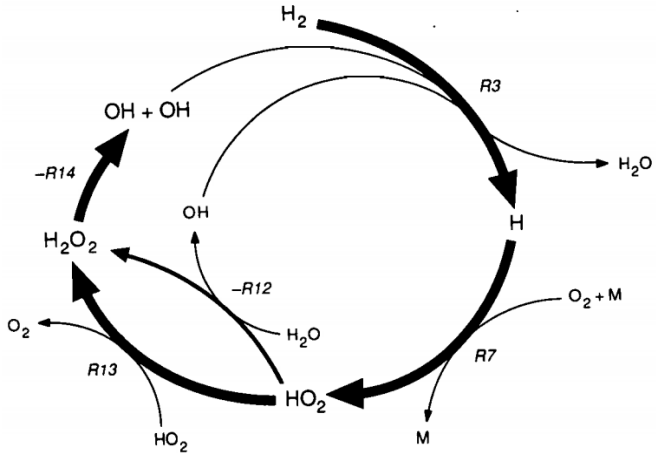

Figure 11. DCKM for hydrogen oxidation in SCW [119].

Table 3. Dominating reactions used in elementary reaction models for hydrogen oxidation in SCW at 246 bars [119].

#	Reaction	$k = AT^b\exp(-E_a/RT)$ [1]			Notes
		A	b	E_a	
1	$H_2+OH\rightarrow H_2O+H$	8.33	1.51	14.35	
2	$H+O_2+M\rightarrow HO_2+M$	16.50	0.0	−4.18	
3	$HO_2+HO_2\rightarrow H_2O_2+O_2$	12.93	0.0	17.62	
4	$H_2O_2+OH\rightarrow H_2O+HO_2$	12.85	0.0	5.98	Reverse reaction dominates
5	$OH+OH\rightarrow H_2O_2$	13.88	−0.37	0.0	Reverse reaction dominates
6	$OH+HO_2\rightarrow H_2O+O_2$	16.16	−1.0	0.0	
7	$H_2O_2+H\rightarrow HO_2+H_2$	13.68	0.0	33.26	Reverse reaction dominates

[1] Units of kJ, mol, cm^3, s, K

Moreover, because the oxidation was greatly inhibited by surface reactions, Holgate and Tester [119] incorporated the surface reactions into model YDR91A to moderate the model's overpredicted oxidation rates and seek better consistency with experimental data. Unexpectedly, models with (YDR91S) and without (YDR91J) surface reactions gave equally good agreement with the experimental data, and the sensitivity analysis of model YDR91S indicated that the oxidation process is highly sensitive to the surface rate constant, which suggested that experiments might be irreproducible, yet the data in their study showed good reproducibility. In their subsequent studies, they investigated the role of water in SCWO by describing the effects of pressure or water density in the quantitative analysis [118]. The high pressure can affect the rate constant of the pressure-dependent reactions, such as the dissociation of hydrogen peroxide ($H_2O_2\rightarrow OH\bullet+OH\bullet$) and the dissociation (recombination) of hydroperoxyl radical ($H\bullet+O_2\rightarrow HO_2\bullet$), which are at or near its high-pressure limit. Additionally, water concentration greatly varies with the change of operating pressure in the unique SCW environment, which led to the greatly accelerated rate of the $HO_2\bullet+H_2O\rightarrow H_2O_2+OH\bullet$ branching reaction and promoted the H_2 formation via $H_2O+H\bullet\rightarrow H_2+OH\bullet$.

Brock and Savage [120] constructed a DCKM to describe the SCWO of CH_4, CH_3OH, CO, and H_2 for the first time, and used the Lindemann model to explain the pressure dependence for unimolecular reactions in their model, improving on previous models [119] that only considered the pressure dependence of a few reactions. The Arrhenius plot indicated that the model shows good agreement for experimental results at high temperatures. However, in all cases, the H_2 concentrations predicted by the model were much lower than the experimental ones while the curve shapes are very similar. Compared to the good prediction of Holgate and Tester's model [119], which may be caused by the fortuitous combination of inaccuracies in the predicted induction times and kinetic decay constants, the model developed by Brock and Savage [120] confirmed the error is caused by the short induction time of the model while the kinetic decay constants maintain a high level of consistency with experimental results.

3.3.2. Methanol

Webley and Tester [121] compared the methanol oxidation in gas-phase and SCW and found no measurable amounts of hydrocarbons yielding in gas-phase methanol oxidation were produced. Additionally, they thought the water-gas shift reaction lead to the production of hydrogen in SCW while Bell and Tipper [127] attributed the formation of hydrogen to the reaction $H\bullet+CH_3OH\rightarrow H_2+CH_2OH\bullet$ in gas-phase. Furthermore, Bell and Tipper [127] found the addition of water effectively increased the rate of methanol oxidation at 440 °C, which may be because the water adsorbed onto the surface of the vessel, covering adsorption sites for oxygen molecules and reducing the rate of chain-termination.

The above results indicate that although the free radical reaction dominates in both the gas-phase and SCW, the reaction mechanism is still quite different.

Brock and Savage's model to describe the SCWO of C1 compounds and H_2 overpredicted the rate constants but underestimated the activation energy [120]. The reason why the model did not perform as well for methanol as it did for methane may be that the methanol experiments were run at lower temperatures. The closer the temperature was to the critical point, the worse the ideal gas approximations used in the model became. Though their model did not fit the experimental results well, it correctly predicted the reaction order for O_2 is zero and for methanol is within experimental uncertainty. Methanol was also one of the products of methane oxidation in SCW in Webley and Tester's study [70], taking a small share (<1%) in the reaction pathways predicted from the DCKM.

Brock et al. [66] established a DCKM of methanol oxidation in SCW and identified the main elementary reaction steps with the largest net rates, as shown in Figure 12. A common theme in the methanol SCWO is that an OH• attacks a stable carbon-containing molecule (CH_3OH, CH_2O, and CO) to form a carbon-containing radical intermediate. Methanol was consumed by OH• in two parallel pathways and transformed into CH_3O or CH_2OH, both of which produced formaldehyde by oxidization: the CH_3O radical reacts mostly by eliminating a hydrogen atom, whereas the CH_2OH radical mostly reacts with O_2. Formaldehyde was mostly attacked by OH• to form HCO radicals, which reacted with O_2 to produce CO subsequently. Then CO reacted with OH• to form HOCO radical and HOCO further combined with O_2 to form CO_2. Furthermore, a sensitivity analysis was conducted to identify the eight reactions with the greatest impact on the concentration of reaction products and intermediates, as shown in Table 4 [66]. The analysis results suggested that the further elementary reaction investigations (particularly at high pressures) of H_2O_2 decomposition, HO_2• auto-reaction and HO_2•+CH_3OH reaction (especially at high pressure) may further improve the predictive power of DCKM. In order to apply the DCKM to supercritical water oxidation reactor engineering studies, Brock et al. reduced the previous methanol oxidation mechanism [66], which contained 151 reactions and 22 species, to a mechanism that comprised only 17 reactions and 14 species [116] by net-rate analysis and sensitivity analysis. The predictions from the reduced model were largely indistinguishable from those of the complete DCKM within a specific region.

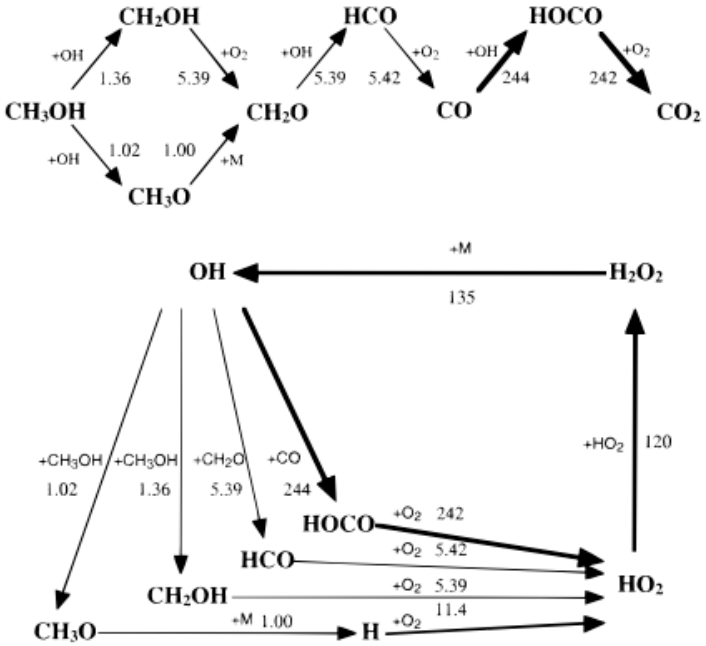

Figure 12. Mainly elementary reaction steps for the SCWO of methanol [66].

Table 4. Reactions with Largest Normalized Sensitivity Coefficients [66].

#	Reaction [1]	Sensitivity Coefficients			
		CH_3OH	CH_2O	CO	CO_2
1	$CH_3OH+OH \rightarrow H_2O+CH_2OH$	−0.101	0.313	0.106	−0.131
2	$CH_3OH+OH \rightarrow H_2O+CH_3O$	−0.074	0.210	0.091	−0.052
3	$CH_3OH+HO_2 \rightarrow H_2O_2+CH_2OH$	−0.224	0.017	0.773	1.47
4	$CH_2O+HO \rightarrow H_2O+HCO$	0.106	−0.535	0.111	−0.151
5	$CH_2O+HO_2 \rightarrow H_2O_2+HCO$	−0.205	−0.106	0.819	1.50
6	$HO_2+HO_2 \rightarrow H_2O_2+O_2$	0.394	0.036	−1.42	−2.74
7	$H_2O_2(+M) \rightarrow HO+HO(+M)$	−0.797	0.042	2.77	5.31
8	$OH+H_2O_2 \rightarrow HO_2+H_2O$	−0.463	0.013	1.62	3.10

[1] For SCWO at 538 °C, 246 atm, 0.7 s, $[H_2O]_0 = 4.49 \times 10^{-3}$, $[O_2]_0 = 4.64 \times 10^{-6}$, and $[CH_3OH]_0 = 7.27 \times 10^{-7}$ (mol/cm^3).

Subsequent studies have further improved the predictive power of the DCKM model. Henrikson et al. [128] updated kinetic parameters and thermodynamic data on the basis of the DCKM of methanol proposed by Brock et al. [66] to analyze the effect of water density on oxidation kinetics, which nicely reproduced the experimental phenomenon of increased reaction rates due to increased water density. Since OH• reaction with methanol is the fastest reaction step for methanol removal, an increase in water density increased the rate of reactions to produce OH• ($H•+H_2O=OH•+H_2$, $CH_3•+H_2O=OH•+CH_4$). Hence, the concentration of OH• increased with the increase of water density, which led to an increase in degradation reaction rate. Tatsuya Fujii et al. [129] combined experiments and the DCKM of methanol improved by Henrikson et al. [128] to investigate the effect of density on methanol oxidation at 420 °C and 34–100 MPa. Different from the study by Henrikson et al. [128], the sensitivity coefficients of the methanol concentration and the rate of OH• production to the water density indicated that the rate of reaction ($HO_2•+H_2O=OH•+H_2O_2$) to produce OH• accelerated under high pressure, which in turn promoted the decomposition of methanol. The difference in the sensitivity analysis was caused by the different water density ranges they studied. The water density under Fujii et al.'s [129] experimental conditions was 3.0–6.6 × 10^2 kg/m^3, which was higher than 1.0×10^2 kg/m^3 in the Henrikson et al.'s [128] experiments. Furthermore, Tatsuya Fujii et al. [129] analyzed the effect of diffusion restriction on the reaction at high water density. In contrast to phenol where the SCWO process would be affected by diffusion to some extent, although the two reactions ($CH_2O+H•\rightarrow CH_2OH$, $H•+O_2(+M)\rightarrow HO_2•$) in the methanol SCWO process would be strongly affected by diffusion restriction, there was essentially no effect on the overall reaction of methanol SCWO.

Recently, Ren et al. [72] supplemented and improved seven important elementary reactions based on the methanol gas-phase combustion mechanism proposed by Li et al. [130] and the studies by Burke [131], Brock [120], Dagaut [132], and Alkam [133], thus correcting for pressure-dependent hydrothermal sensitive reactions. In addition, since the heat released during hydrothermal combustion is much higher than that released in SCWO, the reaction temperature is very sensitive to thermodynamic properties such as heat capacity, enthalpy, etc. Fitting the supercritical state specific heat capacity by a segmented polynomial, the model reliably reflected the changes in species concentration and temperature under hydrothermal conditions. The results showed that high free radical content induced by high methanol concentration was the main factor leading to rapid reaction and flame formation.

3.3.3. Acetic Acid

Boock and Klein proposed a DCKM for the oxidation of acetic acid in SCW using oxygen as an oxidant [31,122]. The DCKM consisted of 19 elementary reactions that were divided into eight reaction families. A reaction family is a set of reactions, which have similar transition states and changes in the reactivities of family members that are largely due to changes in reaction energetics. As a result,

changes in entropies between reactants and transition states in a reaction family are proportional to those in enthalpies. Individual rate constants were estimated by adjusting the pre-exponential factor for steric effects and estimating the activation energies for each elementary reaction, which were constrained to follow simple structure/reactivity correlations. The structure/reactivity model for the oxidation of acetic acid predicted the experimental results well at 350 °C, while underpredicting and overpredicting the data at 350 and 415 °C, respectively. The temperature effect indicated that the refinement of values for the activation energies rather than pre-exponential factors would further increase correlation.

Maharrey et al. [80] coupled a quartz capillary micro-reactor with a mass spectrometer to study the reaction mechanism of acetic acid in the SCWO process, which could detect the intermediates, free radicals and products produced in the early stages of the reaction at conditions above 23 MPa and 400–500 °C. At lower temperatures below 500 °C, SCW was not involved in the reaction and only used to maintain a fully mixed single-phase reaction environment. Furthermore, hydrogen peroxide was completely decomposed to oxygen by 450 °C, whereas subsequent degradation of acetic acid began at 470 °C, which was consistent with the fact that oxidation of acetic acid began primarily by O_2 rather than the extraction of hydrogen from acetic acid by OH•. Zhang et al. [79] also inferred that the decarboxylation of acetic acid could not be carried out through reaction (20), but by the hydrogen extraction reaction by O_2 in reaction (21) to form HO_2•. However, the deduction that acetic acid was more reactive with O_2 rather than HO• may be attributed to oxygen concentration being much higher than HO• concentration in their study [79,80]. Developments in computational chemistry and molecular dynamics will play an important role in predicting the reactivity of O_2 and HO•.

3.3.4. Benzene

DiNaro et al. [102,123] developed an elementary reaction mechanism for benzene oxidation in SCW based on the low-pressure benzene combustion mechanism and submechanisms for the oxidation of key intermediates, which incorporated the aromatic to C-1, C-1, and H_2/O_2 submechanisms. The benzene combustion mechanism was modified critically to meet the lower temperatures and higher pressures of SCWO, including (1) the adaptation of some recombination reactions for pressure; (2) the addition of a pressure-corrected C5H5/C5H6 submechanism; (3) the inclusion of bimolecular reactions and thermal dissociation reactions of C_6H_5OO; and (4) the insertion of reactions for phenyl radical (C_6H_5) degradation and rate coefficients predicted by CHEMDIS.

Figure 13 shows the revised major oxidation pathways of benzene in SCWO [123]. The conversion to C_6H_5 includes principal reactions while C_6H_5OH is minor for benzene decomposition. The model befits the experimental benzene and phenol concentration profiles and predicted the measured benzene conversion accurately, while the predicted CO and CO_2 concentrations were inconsistent with experimental measurement values due to the lack of chemistry for the further oxidation of the linear C_6, C_5, C_4 intermediate species to CO and CO_2. However, the model overcame the problems that the predicted oxidation rate of benzene was too fast and the concentration of CO was incorrectly predicted to exceed that of CO_2 since the two thermal decomposition reactions of C_6H_5OO were inserted.

3.3.5. Ammonia

Nitrogenous organic compounds were common refractory compounds in organic contaminants such as landfill leachate and sewage sludge [68,112,134]. Although the SCWO technology is an efficient water treatment technology that can achieve efficient degradation of organic pollutants and over 99% TOC removal rate, the effluents with high NH_3 content still need further treatment to reach the standard discharge since the destruction of ammonia is the rate-limiting step in the SCWO of nitrogen wastewaters [41,135,136]. Some researchers have investigated the removal of ammonia in typical SCWO conditions (400–700 °C, 24–25 Mpa) and confirmed ammonia is recalcitrant in SCWO [41,137]. For example, Webley et al. reported that only 8.3% ammonia had converted at 680 °C and 246 bar in 10.9 s when the ratio of oxygen and ammonia was 1.266 [41]. To achieve efficient degradation of

NH_3, alcohols such as methanol [38,41,138], ethanol [125,139,140] and IPA [138,141–143] were used in the SCWO treatment of ammonia and the degradation of ammonia could be drastically enhanced by controlling coexisting materials.

Some researchers have developed detailed chemical kinetic models to clarify the effects of alcohols co-oxidation on the SCWO of ammonia and elucidate the reaction mechanisms in detail [124,125]. Ploeger et al. [125] constructed the initial ammonia-ethanol co-oxidation on the basis of the developed MPA-ethanol co-oxidation mechanism [126] composed of ammonia submechanism and ethanol submechanism. Although the initial model underpredicted the conversion of ammonia significantly and predicted the N_2O yields poorly, it is accurate enough to provide a starting point for improvements. Figure 14 shows the predominant reaction pathways in the initial ammonia-ethanol mechanism. The reaction $NO_2\bullet+NH_2\bullet=N_2O+H_2O$ is the dominant pathway forming N_2O and the NO_x submechanism is in a dominant position under co-oxidation conditions. Since H_2NNO_x adducts are more likely to be collision stabilized at high pressures, they were focused on improving the model predictions for ammonia conversion and N_2O yield as the intermediate species of the $NO_x+NH_2\bullet$ reactions. The reaction surface and rearrangement products for the H_2NNO_2 adduct and H_2NNO adduct were calculated using Gaussian [144] software with the CBS-Q method [145] in the updated ammonia–ethanol co-oxidation model. The addition of the H_2NNO_x adduct species have clearly improved the prediction of N_2O yields, and the major reaction pathways for the revised ammonia-ethanol co-oxidation model are shown in Figure 15. However, the updated co-oxidation model cannot correctly reproduce the ammonia conversion trends as a function of temperature in experiments. Further studies of transient species are needed since the formation of the H_2NNO_x and H_2NONO adducts strongly affect the ammonia conversion trends and N_2O production profiles.

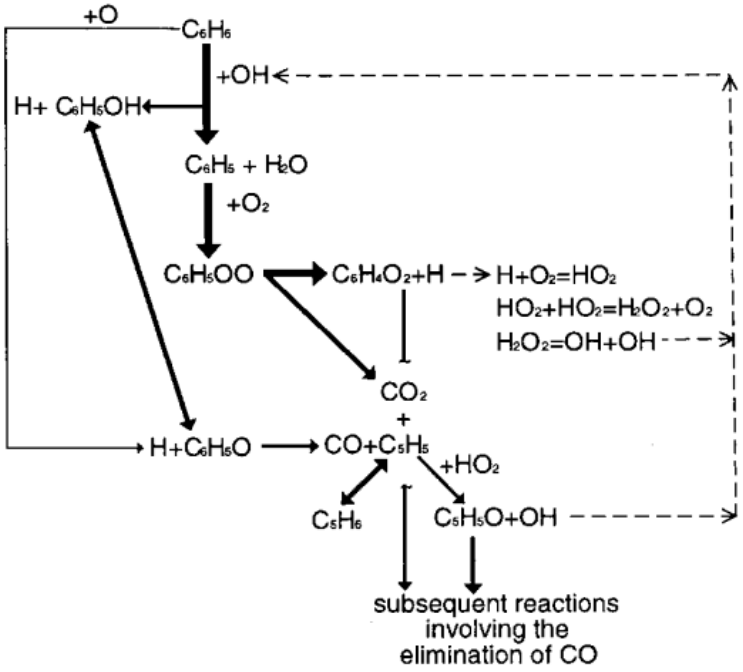

Figure 13. Revised major oxidation pathways of benzene in SCWO [123].

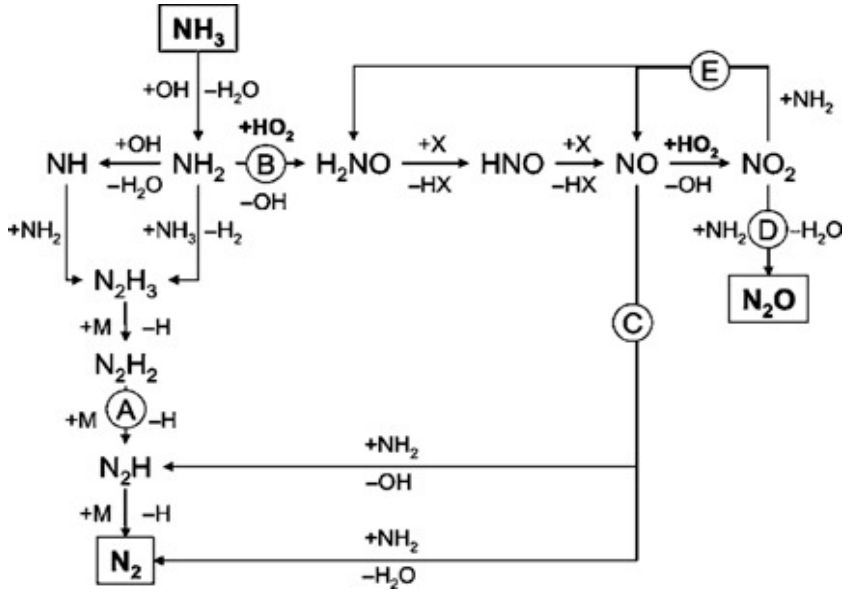

Figure 14. Major reaction pathways for the initial ammonia-ethanol co-oxidation model [125].

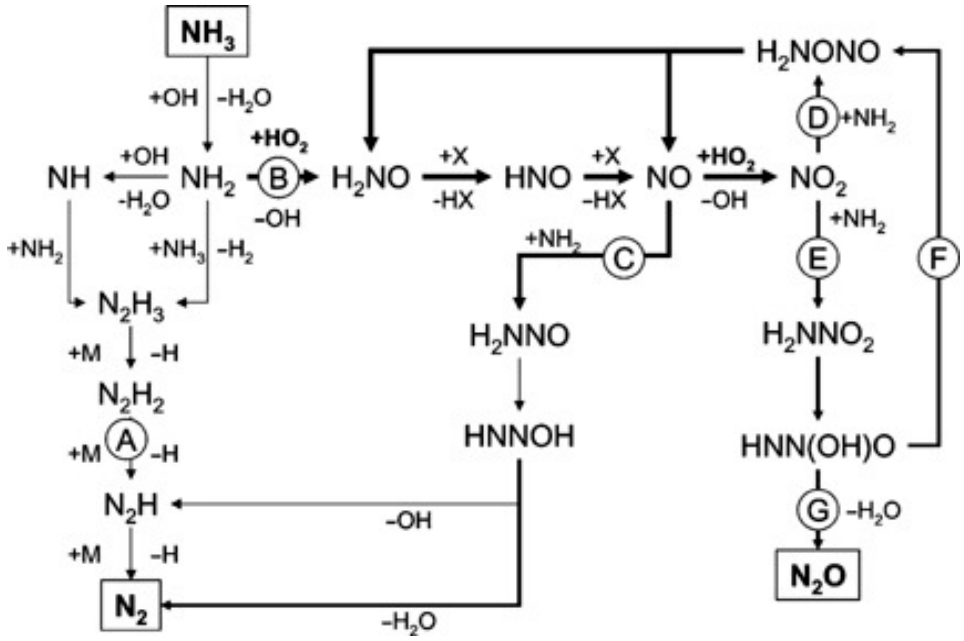

Figure 15. Major reaction pathways for the updated ammonia-ethanol co-oxidation model [125].

Shimoda et al. [124] expounded the effects of methanol co-oxidation on SCWO of ammonia in detail based on the newly-developed elementary reaction model which combined the methylamine oxidation model [146] and ethanol/methanol oxidation model [147]. In the model simulations, the ammonia conversion increased with the increase in initial methanol concentration and the decomposition of methanol and the oxidation of CO mmol/L finished faster when NH_3 existed, which reproduced the phenomenological findings in the experiments. The increase in initial methanol concentration was beneficial to the increase of OH concentration and further accelerated the ammonia decomposition, while the reactions of N-containing species produced OH• and H_2O_2, which also accelerated the methanol decomposition due to the higher OH• concentration in the NH_3/CH_3OH mixture. Regretfully, the conversion and C-based yield of the model simulation results are not in quantitative agreement with the experimental results, because the base model for reactions of nitrogen species is based on the gas-phase kinetics in higher temperatures around 1000 °C, instead of the lower temperature and

a large amount of water used as solvent in conventional SCWO conditions. Recently, Ashraful and Silva [148] proposed an improved DCKM for methylamine oxidation in SCW, in which the peroxyl radical chemistry including imine formation as the main path for amine oxidation was added. Figure 16 demonstrates the major reaction paths in the methylamine SCWO process. The updated model not only clearly described the efficient conversion of CH_3NH_2 to NH_3, but also improved the prediction of CO_2 formation since the rate of the CO+HNO reaction has changed.

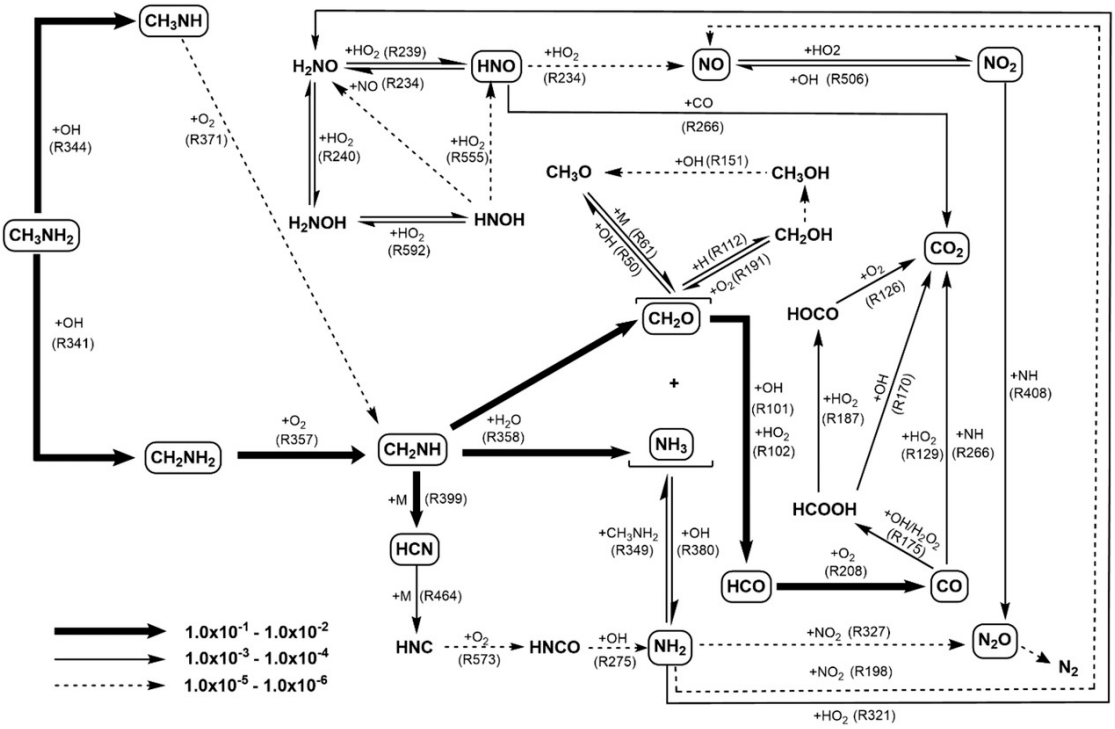

Figure 16. Major reaction pathways for CH_3NH_2 oxidation in SCW [148].

4. Developments of Computational Chemistry

This section mainly retrospected the advances of quantum chemistry and molecular dynamics simulations in the supercritical water oxidation field. With the improvement of molecular microscopic theory, the development of high-performance computing technologies and the rise of new calculation methods, quantum chemistry and molecular dynamics simulations as the auxiliary means of experimental research have been widely concerned by scholars, and have demonstrated their outstanding advantages and guiding significance in the field of theoretical analysis [149]. The profound understanding of the intrinsic processes and dynamics of SCWO reactions plays an important role in constructing a reasonable DCKM, which is necessary for achieving reaction path control and reactor design optimization. Savage and his team have pointed out that the DCKM effectively ties together reaction mechanisms and global dynamics [150]. However, conventional measures are limited due to the high-temperature and high-pressure reaction conditions of SCWO, while quantum chemistry and molecular dynamics simulations can provide new support for understanding the potential role of water and improving the DCKM.

4.1. Quantum Chemistry

Quantum chemistry uses the methods and principles of quantum mechanics to study problems in chemistry. It includes three chemical bonding theories: valence bond theory, molecular orbit theory, and coordination field theory. Quantum chemistry calculations can obtain information on the optimal conformation and transition-state intermediates of reactants and their energy and charge transfer, which are difficult to measure in the laboratory. Thus, they can more accurately explain the mechanism

of chemical reactions, analyze the phenomena from a higher theoretical point of view, and provide a description of the molecular or atomic level. With the rapid development of quantum chemistry in the SCWO process, it has been used to predict reactive sites, analyze structural properties of matter, construct reaction path energies and kinetic modeling, and make qualitative/quantitative description of degradation properties and structural properties of organics.

The calculations of cracking energy and the predictions of reaction sites by quantum chemistry well explained the degradation orders of different groups in SCWO processes. Zhang et al. [151] calculated the cracking energy for 2,4,6-trinitrotoluene (TNT) SCWO using the $Dmol^3$ by Materials Studio [152] software. The DFT calculations demonstrated that C-N bonds had the weakest cracking energy (69.6 and 75.6 kcal/mol) than other kinds of bonds (>95 kcal/mol), which explained that most of the initial reactions are relevant to the $–NO_2$ group. As an important concept in the conceptual density functional theory (DFT) framework, Fukui functions were defined by Parr and Yang in 1984 and have been widely used to predict reaction sites since then [153–155]. It is generally believed that the larger the Fukui indices value, the greater the reactivity of the corresponding site [156]. Yang et al. [37,43] found that the N atom in the $-NH_2$ group was more vulnerable than that in the $-NO_2$ group by calculating Fukui indices for the radical attack, indicating the $-NH_2$ group may be attacked first by hydroxyl radical rather than the $-NO_2$ group. The degradation pathway of BPA was also investigated by calculating the Fukui indices, indicating the hydroxyl groups on the benzene rings were replaced at first, and then the C-C bond between the two aromatic rings was attacked [157].

Tan et al. [158] studied the temperature sensitivity of aromatic compound destruction in the SCWO process by analyzing the correlation coefficients between the highest slope of the temperature-effect curve (i_{max}) and various molecular descriptors calculated by using quantum chemical method. The correlation coefficients revealed that the effect of temperature on organics composition in SCWO was more related to dipole moment (μ), heat of formation (HOF) and most positive partial charge of a hydrogen atom connected to a carbon atom ($q_{C\text{-}H+}$) than other molecular descriptors. Furthermore, Yang et al. [37] explored the relationship between TN removal and molecular structural characteristics of 14 N-containing compounds using the DFT method to calculate molecular descriptors. The most negative partial charge on a carbon atom (q_{C-}), the most positive partial charge of a hydrogen atom connected to a carbon atom ($q_{C\text{-}H+}$), and the maximum values of Fukui indices of OH• radical attack ($F(0)_x$) had great impacts on temperature behavior of TN removal. For the catalytic supercritical water oxidation (CSCWO) process, bond order (BO_n), and the most positive partial charge on a hydrogen atom ($q(H)_x$) largely affected the TOC degradation behaviors [157]. Based on the qualitative analysis of material structures and degradation characteristics, Cheng et al. [159] developed and evaluated two Quantitative-Structure-Activity-Relationship (QASR) models to describe the relationship between quantum parameters and removal behaviors that include the reaction rate constants of total nitrogen (k_{TN}) and the temperature at which the total nitrogen removal efficiency is 50% (T_{TN50}). The degradation behaviors of organics in SCWO could be predicted through quantum parameters by QASR analysis, reducing the need for further experiments to gain optimum reaction conditions.

For the former developed DCKMs in SCWO [119–121], many reaction rates have no reliable, experimentally determined parameters since the experimental measurement is limited by the high temperature and high-pressure conditions of SCWO. Some scholars focus on the quantum chemistry calculations to gain accurate reaction rates [160,161]. Ideally, all reaction rates could be calculated by ab initio transition state theory (TST) calculations and be more accurate than those estimated from general rate estimation methods [160]. Zhang et al. [162] used high-accuracy quantum chemical calculations for the OH•-initiated SCWO reaction of 2-chlorophenol (2-CP) and performed geometry optimizations of the reactants, the product radicals, the pre-reactive and the transitions state complexes with the DFT method. The theoretical calculations showed that OH• adding to the para-C atom of 2-CP was the easiest to occur due to the lowest energy barrier, and was the most favorable process for forming chlorohydroquinone. Although the theoretical results were consistent with the experimental findings

in product distributions, they were not further applied to dynamics modeling since the reactions were simulated in gas conditions.

4.2. Molecular Dynamics

At present, quantum chemistry calculations of high-dimensional reaction potential energy surfaces are limited to very small systems containing 3–6 atoms. Compared with conventional combustion systems, due to the high-pressure environment, the SCWO system, which has complex intermediates and a large scale and often involves adducts, is a serious challenge for building numerical simulations of the reaction mechanism on the quantum chemistry potential energy surface. Additionally, quantum chemical methods require calculations of energy information for each reaction, whose numbers in the actual SCWO process is extremely large, making it difficult to obtain a complete chemical reaction network. However, with the continuous development of molecular force fields, molecular dynamics simulations can give dynamic information about the system, and larger simulated systems can be processed quickly and efficiently. The current force fields used in molecular dynamics simulations are mainly ReaxFF [151,163–165] and COMPASS [166,167].

The active radicals and their sources during the SCWO process were investigated in previous studies [163,165]. Zhang et al. [163] clarified the reaction mechanism of SCWO by tracing the changes of water and oxygen in SCW. OH• radicals could be obtained directly from the decomposition of water clusters and H• radicals were also produced, while HO_2• radicals were produced through two paths: (i) oxygen molecule interacted with H• produced form water cluster, (ii) oxygen molecule took a hydrogen atom away from the organic matter. Whereafter, HO_2• reacted with another H• to form a H_2O_2 molecule. Finally, the H_2O_2 molecule was decomposed into two OH• radicals. In addition, Ma et al. [165] used H_2O_2 as an oxidant to expound the sources of radicals and oxygen by tracing the changes of water and hydrogen peroxide. The transformation path between free radicals and oxidants is shown in Figure 17. Compared with the previous study, the HO_2• can also be produced by the interaction of H_2O_2 with OH•. Meanwhile, O_2 is mainly produced through the interactions between HO_2•, and HO_2• interacting with OH•. OH• is the most effective oxidizer in the SCWO process in their study, which has been demonstrated by the experimental studies of Savage et al. [168].

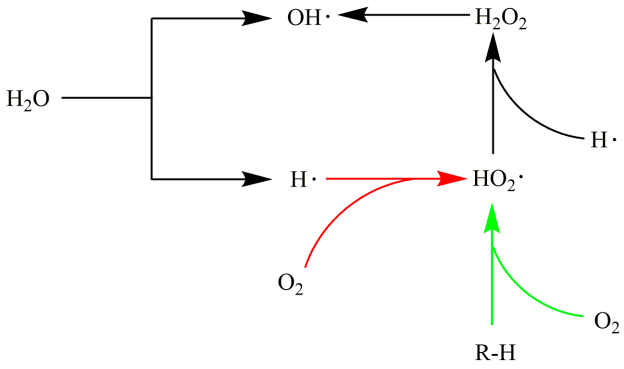

Figure 17. Transformation path between active radicals and oxidants during the SCWO process (Adapted from Ma et al.'s model [165]).

Molecular dynamics simulation is also used to investigate the reaction paths of organics in SCW with/without oxidants. The aromatic ring-opening reaction of disperse orange 25 (DO25) happens mainly through three different pathways since DO25 can be attacked by OH•, O_2, and OH• together with O_2, respectively [163]. Both the OH• radical and O atom promote the ring-opening by weakening the C-C bond in aromatic rings. Ma et al. [165] studied the composition of penicillin (PCN) in SCWO, which consists of the linear-chain cleavage and the ring-opening reactions of two heterocycles and one aromatic ring. Because of the unstable structure of the two adjacent heterocycles, the heterocycles were opened first, and then the linear chain was broken. Zhang et al. [151] used MD simulations

based on the ReaxFF reactive force field to explore the reaction paths of 2,4,6-trinitrotoluene (TNT) in the SCWO process. The initial reaction of TNT oxidation in SCWO included four pathways: (1) $NO_2 \rightarrow ONO$, (2) R-NO_2 bond breaking to produce a NO_2 molecule, (3) R-NO_2 transforming into R-NOOH by the attack of H radicals, and (4) O_2 embedding into the aromatic ring of TNT. In their study [151,163,165], since the C-O bond in the produced ring structure is much weaker than the C-C bond, the ring-opening reactions of the aromatic ring are promoted by embedding O atoms into the aromatic ring.

The different reaction mechanisms of SCWG, SCWO and SCPWO were also discussed through MD simulations. Selecting benzo[a]pyrene (BaP) as a model compound, Jiang et al. [164] found that OH• attack was the main ring-opening reaction mechanism for the SCWG system, while oxygen molecules were dominant in the initial reaction for the SCWO system, and the ring-opening reaction mechanism was initiated by an OH• and oxygen molecules for the SCWPO system. Zhang et al. [151] described the routes of the N element in the whole reactions. The N transformation pathways were similar for SCWG and SCWO, while the final product distributions were obviously different. The intermediate NOH played a key role in the transformation paths and the final products of the N element, which further made NH_3 the main product in the SCWG system and N_2 the primary product in the SCWO system. Jiang et al. [164] optimized the oxygen ration to improve the number of fuel gases using MD simulations. The optimal oxygen ration for maximum H_2 production was 0.2 since adding a small amount of oxygen increased the reaction rate and promoted more H atoms and C atoms to convert into H_2 and CO fuel gases.

Except for the studies of sources of active radicals, reaction paths, migration routes of heteroatoms, and optimization of reaction conditions, some scholars investigated the deposit characteristics and catalytic characteristics of mineral salts in SCWO [166,169]. Zhang et al. [169] investigated the nucleation and growth process of Na_2CO_3 in 1ns computing time at 700–1100 K and 23–30 MPa. The whole nucleation process of Na_2CO_3 was mainly affected by the electrostatic interaction. Since the electrostatic interaction of water molecules with Na^+ and CO_3^{2-} ions rapidly decreased under supercritical conditions, Na_2CO_3 clusters were formed by easy collisions between Na^+ and CO_3^{2-} ions. The higher temperature effectively promoted the ions collision rate and the formation of more initial Na_2CO_3 particles at the nucleation stage. Ma et al. [166] studied the ion association interactions of NaOH and KOH since the dissociations of metal cations and hydroxide ions could accelerate the dechlorination reaction while the ion association interactions could significantly decrease the number of ions and suppress the dechlorination reaction. The simulation results indicated that the ion association interaction decreased with density, but increased with temperature. The effect of KOH was better than that of NaOH, which could be explained by the charge density. The reason behind it is Na^+ with a smaller radius has a bigger charge density.

The microchemical processes for the SCWO of organics can be obtained by using MD simulations based on the reactive force field, which has an important guiding role in constructing the simplified reaction mechanism. The ReaxFF reactive force field is still limited to simulations at high temperatures (e.g., above 3000 K), where reaction times are in the ns order of magnitude and molecular simulations can be achieved at such time scales. However, at real temperature conditions (<1000 K) and reaction times in the s scale, molecular simulation methods are currently unable to achieve simulations on such large time scales. In addition, the reactive force field plays an important role in accurately describing the reaction process, and the development of force fields, which is suitable for SCW conditions, is necessary to improve simulation accuracy.

5. Conclusions and Future Perspectives

SCWO is a promising wastewater treatment technology owing to its various advantages, such as rapid reactions and non-polluting products. However, corrosion, salt deposition, and other problems during the pre-heating stage set obstacles for its commercialization. To address these barriers, a great deal of research has gone into the optimization of reactor design and enhanced SCWO process, which

all require adequate knowledge of reaction kinetics. Well-developed kinetic information can reveal the essence of the SCWO process, which is of sufficient significance for the development of reaction equipment, the setting of operating conditions and the selection of oxidants.

5.1. Applications in Reactor Optimization

Empirical models and semi-empirical models: The reaction kinetics of SCWO has developed from empirical models to semi-empirical models and then to DCKMs. For empirical and semi-empirical models developed based on the experimental results, their wide applications are limited by experimental conditions. Hence, for experimental device amplification, empirical and semi-empirical models can only be used for the amplification of similar reactors in the same experimental range.

DCKM models: Widely available DCKMs are urgently needed for the development of new reactors and the optimization of reactor structures. Since the coupling of complex DCKMs and flow model sharply increased the computing time, the development of simplified mechanism models that are still representative of the chemical reaction process is also an urgent matter. They can substantially reduce the chemical and mathematical complexity of DCKMs. The reduced mechanism eventually makes it possible to use fundamental, mechanism-based kinetics models combined with computational fluid dynamics in reactor engineering studies.

5.2. Applications in Enhanced SCWO Processes

Except for the optimal design of the reactor to make the SCWO system more efficient, enhanced treatments such as co-oxidation with auxiliary fuels, spilt oxidation, hydrothermal combustion and catalyzed oxidation not only make the removal of pollutants more efficient, but also achieve the directional transformation of pollutants. Some scholars have conducted various experimental studied on these enhanced treatments, but their mechanisms still need to be further clarified.

Co-oxidation: the mechanism of producing active free radicals at different temperatures by different auxiliaries is not clear, and the strengthening effect of different additives is still controversial. It is very important to clarify the strengthening mechanism of different auxiliaries and their interaction with temperature in the selection of auxiliaries and temperature in the actual co-oxidation.

Spilt oxidation: how reaction products produced in the first stage of spilt oxidation induce subsequent chemical reaction acceleration remains to be explained. Additionally, the location of oxygen and alcohol injection is also mostly determined by the experiment at present. Developing optimization methods combined with DCKMs and computational fluid dynamics to obtain such an optimal location is necessary for commercial device development.

Hydrothermal combustion: although reactants can be rapidly degraded by high-temperature combustion, the migration of pollutants during combustion still cannot be explained due to the lack of mechanism models, especially the conversion of nitrogen to nitrate.

Catalyzed oxidation: some scholars thought that catalysts produced activated oxygen, such as O_2^-, O and O^{2-}, to promote the removal of organics in the SCWO process [170,171]. However, the DCKMs and detailed kinetic descriptions are still in shortage since the heterogeneous reactions between catalysts and reactants increase the model complexity. Based on the DCKMs of the model compounds, analyzing the mechanisms of each strengthening measure to achieve the directional transformation of pollutants will become a research hotspot in the future.

Both the optimization of the reactor and the development of strengthening measures need to be based on a full understanding of the degradation of reactants, i.e., precise DCKMs are vital for the development of these enhanced treatments. However, most of the detailed chemical kinetic models are developed based on the gas-phase DCKMs since the reaction rates of small molecules reactions in SCWO process are fast due to the high pressure and can be described with a higher reaction constant (high-pressure limit). Hence, for organic compounds such as phenol, which have different reaction mechanisms in SCW and gas-phase, using gas-phase DCKMs to describe the SCWO process has large errors or is even no longer applicable. Relative to gas combustion, the oxidation reactions in SCW occur

at a higher pressure and lower temperature, which need to add some intermediates that are stable in the collision and their reaction paths (e.g., C_6H_5OO in benzene oxidation mechanism). The dynamic parameters of the pressure-dependent reaction under high pressure ($p > 22.1$ MPa) also need to be investigated. With the development of computational chemistry, the specific experimental phenomena in the SCWO process can be well explained by the analysis of material structure characteristics and reactivity site predictions. Much more importantly, SCWO reaction barriers can be analyzed by computational chemistry, which provides the possibility to construct the chemical reaction path conforming to the SCWO environment (low temperature, high pressure, and high water concentration).

Author Contributions: Conceptualization, Z.J. and Y.L.; resources, C.C. and C.Y.; writing—original draft preparation, Z.J.; writing—review and editing, Z.J., Y.L., C.Y., C.C., and J.L.; supervision, S.W. All authors have read and agreed to the published version of the manuscript.

Funding: This study was funded by the National Natural Science Foundation of China (51871179), the National Key Research and Development Program of China (2016YFC0801904), the Fundamental Research Funds for the Central Universities (xjj2018201), the China Postdoctoral Science Foundation (2019TQ0248, 2019M663735), and the Natural Science Foundation of Shaanxi Province (2020JQ-038).

Conflicts of Interest: The authors declare there is no conflicts of interest regarding the publication of this paper.

References

1. Modell, M. Processing Methods for the Oxidation of Organics in Supercritical Water. U.S. Patent 4,338,199, 6 June 1982.
2. Savage, P.E. Organic chemical reactions in supercritical water. *Chem. Rev.* **1999**, *99*, 603–621. [CrossRef] [PubMed]
3. Jiang, C.; Xiao, R.; Yang, P. Research process of advanced oxidation processes in wastewater treatment. *Technol. Water Treat.* **2011**, *37*, 12.
4. Changyuan, T.; Xiaohong, D.; Zuohua, L.; Jun, D.; Renlong, L. Fenton reagents-based AOPs for purification of organic wastewater. *Chem. Res. Appl.* **2007**, *19*, 1177–1180.
5. Garcia-Segura, S.; Ocon, J.D.; Chong, M.N. Electrochemical oxidation remediation of real wastewater effluents—A review. *Process Saf. Environ. Prot.* **2018**, *113*, 48–67. [CrossRef]
6. Bermejo, M.; Cocero, M. Supercritical water oxidation: A technical review. *AIChE J.* **2006**, *52*, 3933–3951. [CrossRef]
7. Vadillo, V.; Sanchez-Oneto, J.; Ramon Portela, J.; Martinez de la Ossa, E.J. Problems in Supercritical Water Oxidation Process and Proposed Solutions. *Ind. Eng. Chem. Res.* **2013**, *52*, 7617–7629. [CrossRef]
8. Veriansyah, B.; Kim, J.-D. Supercritical water oxidation for the destruction of toxic organic wastewaters: A review. *J. Environ. Sci.* **2007**, *19*, 513–522. [CrossRef]
9. Schmieder, H.; Abeln, J. Supercritical water oxidation: State of the art. *Chem. Eng. Technol.* **1999**, *22*, 903–908. [CrossRef]
10. Li, Y.; Wang, S. Supercritical water oxidation for environmentally friendly treatment of organic wastes. In *Advanced Supercritical Fluids Technologies*; Pioro, I.L., Ed.; IntechOpen: London, UK, 2019. [CrossRef]
11. Guiding Opinions of the Ministry of Industry and Information Technology on Accelerating the Advancement of the Development of the Environmental Protection Equipment Manufacturing. Available online: http://www.miit.gov.cn/n1146285/n1146352/n3054355/n3057542/n3057549/c5873558/content.html (accessed on 1 July 2020).
12. Li, Y.; Wang, S.; Sun, P.; Yang, J.; Tang, X.; Xu, D.; Guo, Y.; Yang, J.; Macdonald, D.D. Investigation on early formation and evolution of oxide scales on ferritic–martensitic steels in supercritical water. *Corros. Sci.* **2018**, *135*, 136–146. [CrossRef]
13. Li, Y.; Xu, T.; Wang, S.; Yang, J.; Fekete, B.; Yang, J.; Wu, A.; Qiu, J.; Xu, Y.; Macdonald, D.D. Predictions and analyses on the growth behavior of oxide scales formed on Ferritic–Martensitic in supercritical water. *Oxid. Met.* **2019**, *92*, 27–48. [CrossRef]
14. Li, Y.; Wang, S.; Sun, P.; Xu, D.; Ren, M.; Guo, Y.; Lin, G. Early oxidation mechanism of austenitic stainless steel TP347H in supercritical water. *Corros. Sci.* **2017**, *128*, 241–252. [CrossRef]
15. Yang, J.; Wang, S.; Tang, X.; Wang, Y.; Li, Y. Effect of low oxygen concentration on the oxidation behavior of Ni-based alloys 625 and 825 in supercritical water. *J. Supercrit. Fluids* **2018**, *131*, 1–10. [CrossRef]

16. Li, Y.; Wang, S.; Yang, J.; Xu, D.; Guo, Y.; Qian, L.; Song, W. Corrosion characteristics of a nickel-base alloy C-276 in harsh environments. *Int. J. Hydrog. Energy* **2017**, *42*, 19829–19835. [CrossRef]
17. Li, Y.; Wang, S.; Tang, X.; Xu, D.; Guo, Y.; Zhang, J.; Qian, L. Effects of sulfides on the corrosion behavior of Inconel 600 and Incoloy 825 in supercritical water. *Oxid. Met.* **2015**, *84*, 509–526. [CrossRef]
18. Li, Y.; Wang, S.; Sun, P.; Tong, Z.; Xu, D.; Guo, Y.; Yang, J. Early oxidation of Super304H stainless steel and its scales stability in supercritical water environments. *Int. J. Hydrog. Energy* **2016**, *41*, 15764–15771. [CrossRef]
19. Li, Y.; Macdonald, D.D.; Yang, J.; Qiu, J.; Wang, S. Point defect model for the corrosion of steels in supercritical water: Part I, film growth kinetics. *Corros. Sci.* **2019**, *163*, 108280. [CrossRef]
20. Li, Y.; Wang, S.; Yang, J.; Zhang, Y.; Xu, D.; Guo, Y. Effect of Salt Deposits on Corrosion Behavior of Ni-Based Alloys in Supercritical Water Oxidation of High-Salinity Organic Wastewater. *J. Environ. Eng.* **2019**, *145*, 04019080. [CrossRef]
21. Yang, J.; Wang, S.; Li, Y.; Tang, X.; Wang, Y.; Xu, D.; Guo, Y. Effect of salt deposit on corrosion behavior of Ni-based alloys and stainless steels in supercritical water. *J. Supercrit. Fluids* **2019**, *152*, 104570. [CrossRef]
22. Brunner, G. Near and supercritical water. Part II: Oxidative processes. *J. Supercrit. Fluids* **2009**, *47*, 382–390. [CrossRef]
23. Kritzer, P.; Dinjus, E. An assessment of supercritical water oxidation (SCWO)—Existing problems, possible solutions and new reactor concepts. *Chem. Eng. J.* **2001**, *83*, 207–214. [CrossRef]
24. Xu, D.H.; Huang, C.B.; Wang, S.Z.; Lin, G.K.; Guo, Y. Salt deposition problems in supercritical water oxidation. *Chem. Eng. J.* **2015**, *279*, 1010–1022. [CrossRef]
25. Zhang, S.J.; Zhang, Z.H.; Zhao, R.; Gu, J.J.; Liu, J.; Ormeci, B.; Zhang, J.L. A Review of Challenges and Recent Progress in Supercritical Water Oxidation of Wastewater. *Chem. Eng. Commun.* **2017**, *204*, 265–282. [CrossRef]
26. Qian, L.L.; Wang, S.Z.; Xu, D.H.; Guo, Y.; Tang, X.Y.; Wang, L.S. Treatment of municipal sewage sludge in supercritical water: A review. *Water Res.* **2016**, *89*, 118–131. [CrossRef]
27. Watanabe, M.; Sato, T.; Inomata, H.; Smith, R.L.; Arai, K.; Kruse, A.; Dinjus, E. Chemical Reactions of C1 Compounds in Near-Critical and Supercritical Water. *Chem. Rev.* **2004**, *104*, 5803–5822. [CrossRef] [PubMed]
28. Vogel, F.; Blanchard, J.L.D.; Marrone, P.A.; Rice, S.F.; Webley, P.A.; Peters, W.A.; Smith, K.A.; Tester, J.W. Critical review of kinetic data for the oxidation of methanol in supercritical water. *J. Supercrit. Fluids* **2005**, *34*, 249–286. [CrossRef]
29. Gutiérrez Ortiz, F.J.; Kruse, A. The use of process simulation in supercritical fluids applications. *React. Chem. Eng.* **2020**, *5*, 424–451. [CrossRef]
30. Li, L.; Chen, P.; Gloyna, E.F. Generalized kinetic model for wet oxidation of organic compounds. *AIChE J.* **1991**, *37*, 1687–1697. [CrossRef]
31. Boock, L.T.; Klein, M.T. Lumping strategy for modeling the oxidation of C1-C3 alcohols and acetic-acid in high-temperature water. *Ind. Eng. Chem. Res.* **1993**, *32*, 2464–2473. [CrossRef]
32. Rice, S. Kinetics of Supercritical Water Oxidation-SERDP Compliance Technical Thrust Area. Available online: https://apps.dtic.mil/sti/pdfs/ADA406128.pdf (accessed on 1 July 2020).
33. Martino, C.J.; Savage, P.E. Supercritical water oxidation kinetics, products, and pathways for CH3- and CHO-substituted phenols. *Ind. Eng. Chem. Res.* **1997**, *36*, 1391–1400. [CrossRef]
34. Martino, C.J.; Savage, P.E. Supercritical Water Oxidation Kinetics and Pathways for Ethylphenols, Hydroxyacetophenones, and Other Monosubstituted Phenols. *Ind. Eng. Chem. Res.* **1999**, *38*, 1775–1783. [CrossRef]
35. Jin, F.M.; Moriya, T.; Enomoto, H. Oxidation reaction of high molecular weight carboxylic acids in supercritical water. *Environ. Sci. Technol.* **2003**, *37*, 3220–3231. [CrossRef] [PubMed]
36. Marrone, P.A. Supercritical water oxidation—Current status of full-scale commercial activity for waste destruction. *J. Supercrit. Fluids* **2013**, *79*, 283–288. [CrossRef]
37. Yang, B.W.; Shen, Z.M.; Cheng, Z.W.; Ji, W.C. Total nitrogen removal, products and molecular characteristics of 14 N-containing compounds in supercritical water oxidation. *Chemosphere* **2017**, *188*, 642–649. [CrossRef] [PubMed]
38. Oe, T.; Suzugaki, H.; Naruse, I.; Quitain, A.T.; Daimon, H.; Fujie, K. Role of methanol in supercritical water oxidation of ammonia. *Ind. Eng. Chem. Res.* **2007**, *46*, 3566–3573. [CrossRef]
39. Aki, S.; Abraham, M.A. Catalytic supercritical water oxidation of pyridine: Comparison of catalysts. *Ind. Eng. Chem. Res.* **1999**, *38*, 358–367. [CrossRef]

40. Al-Duri, B.; Alsoqyani, F. Supercritical water oxidation (SCWO) for the removal of nitrogen containing heterocyclic waste hydrocarbons. Part II: System kinetics. *J. Supercrit. Fluids* **2017**, *128*, 412–418. [CrossRef]
41. Webley, P.A.; Tester, J.W.; Holgate, H.R. Oxidation kinetics of ammonia and ammonia-methanol mixtures in supercritical water in the temperature range 530–700°C at 246 bar. *Ind. Eng. Chem. Res.* **1991**, *30*, 1745–1754. [CrossRef]
42. Scandelai, A.P.J.; Zotesso, J.P.; Jegatheesan, V.; Cardozo, L.; Tavares, C.R.G. Intensification of supercritical water oxidation (SCWO) process for landfill leachate treatment through ion exchange with zeolite. *Waste Manag.* **2020**, *101*, 259–267. [CrossRef]
43. Yang, B.; Cheng, Z.; Fan, M.; Jia, J.; Yuan, T.; Shen, Z. Supercritical water oxidation of 2-, 3- and 4-nitroaniline: A study on nitrogen transformation mechanism. *Chemosphere* **2018**, *205*, 426–432. [CrossRef]
44. Killilea, W.R.; Swallow, K.C.; Hong, G.T. The fate of nitrogen in supercritical-water oxidation. *J. Supercrit. Fluids* **1992**, *5*, 72–78. [CrossRef]
45. Tan, Y.J.; Yang, B.W.; Gao, X.P.; Cheng, Z.W.; Liu, S.Q.; Liu, Y.W.; Shen, Z.M. A novel synergistic denitrification mechanism during supercritical water oxidation. *Chem. Eng. J.* **2020**, *382*, 13. [CrossRef]
46. Zhang, J.; Wang, S.Z.; Ren, M.M.; Lu, J.L.; Chen, S.L.; Zhang, H.M. Effect Mechanism of Auxiliary Fuel in Supercritical Water: A Review. *Ind. Eng. Chem. Res.* **2019**, *58*, 1480–1494. [CrossRef]
47. Anitescu, G.; Munteanu, V.; Tavlarides, L.L. Co-oxidation effects of methanol and benzene on the decomposition of 4-chlorobiphenyl in supercritical water. *J. Supercrit. Fluids* **2005**, *33*, 139–147. [CrossRef]
48. Anitescu, G.; Tavlarides, L.L. Methanol as a cosolvent and rate-enhancer for the oxidation kinetics of 3,3′,4,4′-tetrachlorobiphenyl decomposition in supercritical water. *Ind. Eng. Chem. Res.* **2002**, *41*, 9–21. [CrossRef]
49. Franck, E.U. Physicochemical properties of supercritical solvents. *Ber. Der Bunsen Ges. Phys. Chem. Chem. Phys.* **1984**, *88*, 820–825. [CrossRef]
50. Bennett, G.E.; Rossky, P.J.; Johnston, K.P. Continuum Electrostatics Model for an SN2 Reaction in Supercritical Water. *J. Phys. Chem.* **1995**, *99*, 16136–16143. [CrossRef]
51. Balbuena, P.B.; Johnston, K.P.; Rossky, P.J. Computer Simulation Study of an SN2 Reaction in Supercritical Water. *J. Phys. Chem.* **1995**, *99*, 1554–1565. [CrossRef]
52. Akiya, N.; Savage, P.E. Effect of water density on hydrogen peroxide dissociation in supercritical water. 1. Reaction equilibrium. *J. Phys. Chem. A* **2000**, *104*, 4433–4440. [CrossRef]
53. Dileo, G.J.; Neff, M.E.; Savage, P.E. Gasification of guaiacol and phenol in supercritical water. *Energy Fuels* **2007**, *21*, 2340–2345. [CrossRef]
54. Guo, Y.; Wang, S.Z.; Yeh, T.; Savage, P.E. Catalytic gasification of indole in supercritical water. *Appl. Catal. B Environ.* **2015**, *166*, 202–210. [CrossRef]
55. Zhu, C.; Guo, L.J.; Jin, H.; Ou, Z.S.; Wei, W.W.; Huang, J.B. Gasification of guaiacol in supercritical water: Detailed reaction pathway and mechanisms. *Int. J. Hydrog. Energy* **2018**, *43*, 14078–14086. [CrossRef]
56. Song, W.H.; Wang, S.Z.; Guo, Y.; Xu, D.H. Bio-oil production from hydrothermal liquefaction of waste Cyanophyta biomass: Influence of process variables and their interactions on the product distributions. *Int. J. Hydrog. Energy* **2017**, *42*, 20361–20374. [CrossRef]
57. Xu, D.H.; Lin, G.K.; Ma, Z.J.; Guo, Y.; Farooq, M.U.; Wang, S.Z. Partial oxidative gasification of sewage sludge in supercritical water with multi-component catalyst. *Chem. Eng. Res. Des.* **2017**, *124*, 145–151. [CrossRef]
58. Wang, Y.Z.; Zhu, Y.T.; Liu, Z.A.; Wang, L.B.; Xu, D.H.; Fang, C.Q.; Wang, S.Z. Catalytic performances of Ni-based catalysts on supercritical water gasification of phenol solution and coal-gasification wastewater. *Int. J. Hydrog. Energy* **2019**, *44*, 3470–3480. [CrossRef]
59. Xu, D.H.; Guo, S.W.; Liu, L.; Lin, G.K.; Wu, Z.Q.; Guo, Y.; Wang, S.Z. Heterogeneous catalytic effects on the characteristics of water-soluble and water-insoluble biocrudes in chlorella hydrothermal liquefaction. *Appl. Energy* **2019**, *243*, 165–174. [CrossRef]
60. Xu, D.H.; Wang, Y.; Lin, G.K.; Guo, S.W.; Wang, S.Z.; Wu, Z.Q. Co-hydrothermal liquefaction of microalgae and sewage sludge in subcritical water: Ash effects on bio-oil production. *Renew. Energy* **2019**, *138*, 1143–1151. [CrossRef]
61. Cheng, S.N.; Wilks, C.; Yuan, Z.S.; Leitch, M.; Xu, C.B. Hydrothermal degradation of alkali lignin to bio-phenolic compounds in sub/supercritical ethanol and water-ethanol co-solvent. *Polym. Degrad. Stab.* **2012**, *97*, 839–848. [CrossRef]

62. Tester, J.W.; Webly, P.A.; Holgate, H.R. Revised global kinetic measurements of methanol oxidation in supercritical water. *Ind. Eng. Chem. Res.* **1993**, *32*, 236–239. [CrossRef]
63. Lee, G.; Nunoura, T.; Matsumura, Y.; Yamamoto, K. Comparison of the effects of the addition of NaOH on the decomposition of 2-chlorophenol and phenol in supercritical water and under supercritical water oxidation conditions. *J. Supercrit. Fluids* **2002**, *24*, 239–250. [CrossRef]
64. Meyer, J.C.; Marrone, P.A.; Tester, J.W. Acetic-acid oxidation and hydrolysis in supercritical water. *AIChE J.* **1995**, *41*, 2108–2121. [CrossRef]
65. Schanzenbächer, J.; Taylor, J.D.; Tester, J.W. Ethanol oxidation and hydrolysis rates in supercritical water. *J. Supercrit. Fluids* **2002**, *22*, 139–147. [CrossRef]
66. Brock, E.E.; Oshima, Y.; Savage, P.E.; Barker, J.R. Kinetics and mechanism of methanol oxidation in supercritical water. *J. Phys. Chem.* **1996**, *100*, 15834–15842. [CrossRef]
67. Krammer, P.; Vogel, H. Hydrolysis of esters in subcritical and supercritical water. *J. Supercrit. Fluids* **2000**, *16*, 189–206. [CrossRef]
68. Gong, Y.; Guo, Y.; Wang, S.; Song, W.; Xu, D. Supercritical water oxidation of quinazoline: Reaction kinetics and modeling. *Water Res.* **2017**, *110*, 56–65. [CrossRef]
69. Henrikson, J.T.; Chen, Z.; Savage, P.E. Inhibition and acceleration of phenol oxidation by supercritical water. *Ind. Eng. Chem. Res.* **2003**, *42*, 6303–6309. [CrossRef]
70. Webley, P.A.; Tester, J.W. Fundamental kinetics of methane oxidation in supercritical water. *Energy Fuels* **1991**, *5*, 411–419. [CrossRef]
71. Zhang, J.; Wang, S.Z.; Xu, D.H.; Guo, Y.; Ren, M.M.; Lu, J.L. Kinetics study on hydrothermal combustion of methanol in supercritical water. *Chem. Eng. Res. Des.* **2015**, *98*, 220–230. [CrossRef]
72. Ren, M.; Wang, S.; Zhang, J.; Guo, Y.; Xu, D.; Wang, Y. Characteristics of Methanol Hydrothermal Combustion: Detailed Chemical Kinetics Coupled with Simple Flow Modeling Study. *Ind. Eng. Chem. Res.* **2017**, *56*, 5469–5478. [CrossRef]
73. Lee, D.S.; Gloyna, E.F.; Li, L. Efficiency of H_2O_2 and O_2 in supercritical water oxidation of 2,4-dichlorophenol and acetic acid. *J. Supercrit. Fluids* **1990**, *3*, 249–255. [CrossRef]
74. Phenix, B.D.; Dinaro, J.L.; Tester, J.W.; Howard, J.B.; Smith, K.A. The Effects of Mixing and Oxidant Choice on Laboratory-Scale Measurements of Supercritical Water Oxidation Kinetics. *Ind. Eng. Chem. Res.* **2002**, *41*, 624–631. [CrossRef]
75. Takagi, J.; Ishigure, K. Thermal decomposition of hydrogen peroxide and its effect on reactor water monitoring of boiling water reactors. *Nucl. Sci. Eng.* **1985**, *89*, 177–186. [CrossRef]
76. Tsang, W.; Hampson, R.F. Chemical Kinetic Data Base for Combustion Chemistry. Part I. Methane and Related Compounds. *J. Phys. Chem. Ref. Data* **1986**, *15*, 1087. [CrossRef]
77. Xiang, B.; Wang, T.; Shen, Z. Supercritical water oxidation kinetics and mechanism of ethanol wastewater. *J. Chem. Ind. Eng.* **2003**, *54*, 80–85.
78. Bourhis, A.L.; Swallow, K.C.; Hong, G.T.; Killilea, W.R. The Use of Rate Enhancers in Supercritical Water Oxidation. *ACS Sym.* **1995**, *23*, 338–347.
79. Zhang, J.; Wang, S.; Guo, Y.; Xu, D.; Li, X.; Tang, X. Co-Oxidation Effects of Methanol on Acetic Acid and Phenol in Supercritical Water. *Ind. Eng. Chem. Res.* **2013**, *52*, 10609–10618. [CrossRef]
80. Maharrey, S.P.; Miller, D.R. A direct sampling mass spectrometer investigation of oxidation mechanisms for acetic acid in supercritical water. *J. Phys. Chem. A* **2001**, *105*, 5860–5867. [CrossRef]
81. Vadillo, V.; Sánchezoneto, J.; Portela, J.R.; de la Ossa, E.J.M. Supercritical Water Oxidation for Wastewater Destruction with Energy Recovery. In *Supercritical Fluid Technology for Energy and Environmental Applications*; Elsevier: Amsterdam, The Netherlands, 2014; Chapter 9, pp. 181–190.
82. Sanchez-Oneto, J.; Portela, J.R.; Nebot, E.; de la Ossa, E.M. Hydrothermal oxidation: Application to the treatment of different cutting fluid wastes. *J. Hazard. Mater.* **2007**, *144*, 639–644. [CrossRef]
83. Anitescu, G.; Zhang, Z.; Tavlarides, L.L. A Kinetic Study of Methanol Oxidation in Supercritical Water. *Ind. Eng. Chem. Res.* **1999**, *38*, 2231–2237. [CrossRef]
84. Mateos, D.; Portela, J.R.; Mercadier, J.; Marias, F.; Marraud, C.; Cansell, F. New approach for kinetic parameters determination for hydrothermal oxidation reaction. *J. Supercrit. Fluids* **2005**, *34*, 63–70. [CrossRef]
85. Portela, J.R.; Nebot, E.; Martín ez de la Ossa, E. Kinetic comparison between subcritical and supercritical water oxidation of phenol. *Chem. Eng. J.* **2001**, *81*, 287–299. [CrossRef]

86. Sánchez-Oneto, J.; Mancini, F.; Portela, J.R.; Nebot, E.; Cansell, F.; Martínez de la Ossa, E.J. Kinetic model for oxygen concentration dependence in the supercritical water oxidation of an industrial wastewater. *Chem. Eng. J.* **2008**, *144*, 361–367. [CrossRef]
87. Jimenez-Espadafor, F.; Portela, J.R.; Vadillo, V.; Sánchez-Oneto, J.; Becerra Villanueva, J.A.; Torres García, M.; Martínez de la Ossa, E.J. Supercritical Water Oxidation of Oily Wastes at Pilot Plant: Simulation for Energy Recovery. *Ind. Eng. Chem. Res.* **2011**, *50*, 775–784. [CrossRef]
88. Abelleira, J.; Sánchez-Oneto, J.; Portela, J.R.; Martínez de la Ossa, E.J. Kinetics of supercritical water oxidation of isopropanol as an auxiliary fuel and co-fuel. *Fuel* **2013**, *111*, 574–583. [CrossRef]
89. Reinhart, D.R.; AlYousfi, A.B. The impact of leachate recirculation on municipal solid waste landfill operating characteristics. *Waste Manag. Res.* **1996**, *14*, 337–346. [CrossRef]
90. Kalinichev, A.G.; Bass, J.D. Hydrogen bonding in supercritical water. 2. Computer simulations. *J. Phys. Chem. A* **1997**, *101*, 9720–9727. [CrossRef]
91. Antal, M.J.; Brittain, A.; Dealmeida, C.; Ramayya, S.; Roy, J.C. Heterolysis and Homolysis in Supercritical Water. *ACS Sym. Ser.* **1987**, *329*, 77–86.
92. Mizan, T.I.; Savage, P.E.; Ziff, R.M. Temperature dependence of hydrogen bonding in supercritical water. *J. Phys. Chem.* **1996**, *100*, 403–408. [CrossRef]
93. Kritzer, P.; Boukis, N.; Dinjus, E. Corrosion of alloy 625 in aqueous solutions containing chloride and oxygen. *Corrosion* **1998**, *54*, 824–834. [CrossRef]
94. Kriksunov, L.B.; Macdonald, D.D. Potential-pH diagrams for iron in supercritical water. *Corrosion* **1997**, *53*, 605–611. [CrossRef]
95. Gong, Y.; Wang, S.; Xu, H.; Guo, Y.; Tang, X. Partial oxidation of landfill leachate in supercritical water: Optimization by response surface methodology. *Waste Manag.* **2015**, *43*, 343–352. [CrossRef]
96. Wang, Y.; Wang, S.; Guo, Y.; Xu, D.; Gong, Y.; Tang, X.; Zhang, J. Oxidative degradation of lurgi coal gasification wastewater: Optimization using response surface methodology. *Environ. Prog. Sustain. Energy* **2014**, *33*, 1258–1265. [CrossRef]
97. Zhang, J.; Wang, S.; Guo, Y.; Xu, D.; Gong, Y.; Tang, X. Experimental study on supercritical water oxidation of CI Reactive Orange 7 dye wastewater using response surface methodology. *Color. Technol.* **2012**, *128*, 323–330. [CrossRef]
98. Xu, S.K.; Butler, I.; Gokalp, I.; Kozinski, J.A. Evolution of naphthalene and its intermediates during oxidation in subcritical/supercritical water. *Proc. Combust. Inst.* **2011**, *33*, 3185–3194. [CrossRef]
99. Helling, R.K.; Tester, J.W. Oxidation kinetics of carbon monoxide in supercritical water. *Energy Fuels* **1987**, *1*, 417–423. [CrossRef]
100. Yong, T.L.K.; Matsumura, Y. Kinetics analysis of phenol and benzene decomposition in supercritical water. *J. Supercrit. Fluids* **2014**, *87*, 73–82. [CrossRef]
101. Yong, T.L.K.; Matsumura, Y. Reaction Pathways of Phenol and Benzene Decomposition in Supercritical Water Gasification. *J. Jpn. Pet. Inst.* **2013**, *56*, 331–343. [CrossRef]
102. Dinaro, J.L.; Howard, J.B.; Green, W.H.; Tester, J.W.; Bozzelli, J.W. Analysis of an elementary reaction mechanism for benzene oxidation in supercritical water. *Proc. Combust. Inst.* **2000**, *28*, 1529–1536. [CrossRef]
103. Gopalan, S.; Savage, P.E. Reaction-mechanism for phenol oxidation in supercritical water. *J. Phys. Chem.* **1994**, *98*, 12646–12652. [CrossRef]
104. Colussi, A.J.; Zabel, F.; Benson, S.W. Very low-pressure pyrolysis of phenyl ethyl ether, phenyl allyl ether, and benzyl methyl-ether and enthalpy of formation of phenoxy radical. *Int. J. Chem. Kinet.* **1977**, *9*, 161–178. [CrossRef]
105. Bamford, C.H.; Compton, R.; Tipper, C. *Liquid Phase Oxidation*; Elsevier: Amsterdam, The Netherlands, 1980; Volume 16.
106. Matsumura, Y.; Nunoura, T.; Urase, T.; Yamamoto, K. Supercritical water oxidation of high concentrations of phenol. *J. Hazard. Mater.* **2000**, *73*, 245–254. [CrossRef]
107. Guan, Q.; Wei, C.; Chai, X.-S. Pathways and kinetics of partial oxidation of phenol in supercritical water. *Chem. Eng. J.* **2011**, *175*, 201–206. [CrossRef]
108. Onwudili, J.A.; Williams, P.T. Reaction mechanisms for the hydrothermal oxidation of petroleum derived aromatic and aliphatic hydrocarbons. *J. Supercrit. Fluids* **2007**, *43*, 81–90. [CrossRef]
109. Anitescu, G.; Tavlarides, L.L. Oxidation of Biphenyl in Supercritical Water: Reaction Kinetics, Key Pathways, and Main Products. *Ind. Eng. Chem. Res.* **2005**, *44*, 1226–1232. [CrossRef]

110. Xu, S.K.; Fang, Z.; Kozinski, J.A. Oxidation of naphthalene in supercritical water up to 420 °C and 30 MPa. *Combust. Sci. Technol.* **2003**, *175*, 291–318. [CrossRef]
111. Crain, N.; Tebbal, S.; Li, L.X.; Gloyna, E.F. Kinetics and reaction pathways of pyridine oxidation in supercritical water. *Ind. Eng. Chem. Res.* **1995**, *34*, 1499. [CrossRef]
112. Gong, Y.; Guo, Y.; Wang, S.; Song, W. Supercritical water oxidation of Quinazoline: Effects of conversion parameters and reaction mechanism. *Water Res.* **2016**, *100*, 116–125. [CrossRef]
113. Joule, J.A.; Mills, K. *Heterocyclic Chemistry*, 5th ed.; Wiley: Hoboken, NJ, US, 2010.
114. Ren, M.M.; Wang, S.Z.; Yang, C.; Xu, H.T.; Guo, Y.; Roekaerts, D. Supercritical water oxidation of quinoline with moderate preheat temperature and initial concentration. *Fuel* **2019**, *236*, 1408–1414. [CrossRef]
115. Li, G.; Lu, Y. Oxidative degradation of quinazoline in supercritical water: A combined ReaxFF and DFT study. *Mol. Simul.* **2018**, *44*, 1508–1519. [CrossRef]
116. Brock, E.E.; Savage, P.E.; Barker, J.R. A reduced mechanism for methanol oxidation in supercritical water. *Chem. Eng. Sci.* **1998**, *53*, 857–867. [CrossRef]
117. Hong, G.T.; Fowler, P.K.; Killilea, W.R.; Swallow, K.C. Supercritical Water Oxidation: Treatment of Human Waste and System Configuration Tradeoff Study. *SAE Tech. Pap.* **1987**, 871444. [CrossRef]
118. Holgate, H.R.; Tester, J.W. Oxidation of hydrogen and carbon-monoxide in subcritical and supercritical water—Reaction-kinetics, pathways, and water-density effects. 2. elementary reaction modeling. *J. Phys. Chem.* **1994**, *98*, 810–822. [CrossRef]
119. Holgate, H.R.; Tester, J.W. Fundamental kinetics and mechanisms of hydrogen oxidation in supercritical water. *Combust. Sci. Technol.* **1993**, *88*, 369–397. [CrossRef]
120. Brock, E.E.; Savage, P.E. Detailed chemical kinetics model for supercritical water oxidation of C1 compounds and H2. *AIChE J.* **1995**, *41*, 1874–1888. [CrossRef]
121. Webley, P.A.; Tester, J.W. *Fundamental Kinetics of Methanol Oxidation in Supercritical Water*; ACS Publications: Washington, DC, USA, 1989.
122. Boock, L.T.; Klein, M.T. Experimental kinetics and mechanistic modeling of the oxidation of simple mixtures in near-critical water. *Ind. Eng. Chem. Res.* **1994**, *33*, 2554–2562. [CrossRef]
123. DiNaro, J.L.; Howard, J.B.; Green, W.H.; Tester, J.W.; Bozzelli, J.W. Elementary reaction mechanism for benzene oxidation in supercritical water. *J. Phys. Chem. A* **2000**, *104*, 10576–10586. [CrossRef]
124. Shimoda, E.; Fujii, T.; Hayashi, R.; Oshima, Y. Kinetic analysis of the mixture effect in supercritical water oxidation of ammonia/methanol. *J. Supercrit. Fluids* **2016**, *116*, 232–238. [CrossRef]
125. Ploeger, J.M.; Green, W.H.; Tester, J.W. Co-oxidation of ammonia and ethanol in supercritical water, part 2: Modeling demonstrates the importance of H_2NNO_x. *Int. J. Chem. Kinet.* **2008**, *40*, 653–662. [CrossRef]
126. Ploeger, J.M.; Green, W.H.; Tester, J.W. Co-oxidation of methylphosphonic acid and ethanol in supercritical water—II: Elementary reaction rate model. *J. Supercrit. Fluids* **2006**, *39*, 239–245. [CrossRef]
127. Bell, K.M.; Tipper, C.F.H. The Slow Combustion of Methyl Alcohol. A General Investigation. *Proc. R. Soc. Lond.* **1956**, *238*, 256–268.
128. Henrikson, J.T.; Grice, C.R.; Savage, P.E. Effect of water density on methanol oxidation kinetics in supercritical water. *J. Phys. Chem. A* **2006**, *110*, 3627–3632. [CrossRef] [PubMed]
129. Fujii, T.; Hayashi, R.; Kawasaki, S.; Suzuki, A.; Oshima, Y. Water density effects on methanol oxidation in supercritical water at high pressure up to 100 MPa. *J. Supercrit. Fluids* **2011**, *58*, 142–149. [CrossRef]
130. Li, J.; Zhao, Z.W.; Kazakov, A.; Chaos, M.; Dryer, F.L.; Scire, J.J. A comprehensive kinetic mechanism for CO, CH2O, and CH3OH combustion. *Int. J. Chem. Kinet.* **2007**, *39*, 109–136. [CrossRef]
131. Burke, M.P.; Chaos, M.; Ju, Y.G.; Dryer, F.L.; Klippenstein, S.J. Comprehensive H_2/O_2 kinetic model for high-pressure combustion. *Int. J. Chem. Kinet.* **2012**, *44*, 444–474. [CrossRef]
132. Dagaut, P.; Cathonnet, M.; Boettner, J.C. Chemical kinetic modeling of the supercritical-water oxidation of methanol. *J. Supercrit. Fluids* **1996**, *9*, 33–42. [CrossRef]
133. Alkam, M.K.; Pai, V.M.; Butler, P.B.; Pitz, W.J. Methanol and hydrogen oxidation kinetics in water at supercritical states. *Combust. Flame* **1996**, *106*, 110–130. [CrossRef]
134. Qian, L.L.; Wang, S.Z.; Ren, M.M.; Wang, S. Co-oxidation effects and mechanisms between sludge and alcohols (methanol, ethanol and isopropanol) in supercritical water. *Chem. Eng. J.* **2019**, *366*, 223–234. [CrossRef]

135. Cocero, M.J.; Alonso, E.; Torio, R.; Vallelado, D.; Fdz-Polanco, F. Supercritical water oxidation in a pilot plant of nitrogenous compounds: 2-propanol mixtures in the temperature range 500–750 °C. *Ind. Eng. Chem. Res.* **2000**, *39*, 3707–3716. [CrossRef]
136. Proesmans, P.I.; Luan, L.; Buelow, S.J. Hydrothermal oxidation of organic wastes using ammonium nitrate. *Ind. Eng. Chem. Res.* **1997**, *36*, 1559–1566. [CrossRef]
137. Segond, N.; Matsumura, Y.; Yamamoto, K. Determination of ammonia oxidation rate in sub- and supercritical water. *Ind. Eng. Chem. Res.* **2002**, *41*, 6020–6027. [CrossRef]
138. Zhang, J.; Li, P.; Lu, J.; Xin, F.; Zheng, X.; Chen, S. Supercritical water oxidation of ammonia with methanol as the auxiliary fuel: Comparing with isopropanol. *Chem. Eng. Res. Des.* **2019**, *147*, 160–170. [CrossRef]
139. Helling, R.K.; Tester, J.W. Oxidation of simple compounds and mixtures in supercritical water: Carbon monoxide, ammonia and ethanol. *Environ. Sci. Technol.* **1988**, *22*, 1319–1324. [CrossRef]
140. Ploeger, J.M.; Mock, M.A.; Tester, J.W. Cooxidation of ammonia and ethanol in supercritical water, part 1: Experimental results. *AIChE J.* **2007**, *53*, 941–947. [CrossRef]
141. Cabeza, P.; Al-Duri, B.; Bermejo, M.D.; Cocero, M.J. Co-oxidation of ammonia and isopropanol in supercritical water in a tubular reactor. *Chem. Eng. Res. Des.* **2014**, *92*, 2568–2574. [CrossRef]
142. Cabeza, P.; Dolores Bermejo, M.; Jimenez, C.; Jose Cocero, M. Experimental study of the supercritical water oxidation of recalcitrant compounds under hydrothermal flames using tubular reactors. *Water Res.* **2011**, *45*, 2485–2495. [CrossRef] [PubMed]
143. Bermejo, M.D.; Cantero, F.; Cocero, M.J. Supercritical water oxidation of feeds with high ammonia concentrations: Pilot plant experimental results and modeling. *Chem. Eng. J.* **2008**, *137*, 542–549. [CrossRef]
144. Frisch, M.J.; Trucks, G.W.; Schlegel, H.B.; Scuseria, G.E.; Robb, M.A.; Cheeseman, J.R.; Scalmani, G.; Barone, V.; Petersson, G.A.; Nakatsuji, H.; et al. *Gaussian 16*; Revision C.01; Gaussian, Inc.: Wallingford, CT, USA, 2016.
145. Ochterski, J.W.; Petersson, G.A.; Montgomery, J.A., Jr. A complete basis set model chemistry. V. Extensions to six or more heavy atoms. *J. Chem. Phys.* **1996**, *104*, 2598–2619. [CrossRef]
146. Benjamin, K.M.; Savage, P.E. Detailed chemical kinetic modeling of methylamine in supercritical water. *Ind. Eng. Chem. Res.* **2005**, *44*, 9785–9793. [CrossRef]
147. Hayashi, R.; Onishi, M.; Sugiyama, M.; Koda, S.; Oshima, Y. Kinetic analysis on alcohol concentration and mixture effect in supercritical water oxidation of methanol and ethanol by elementary reaction model. *J. Supercrit. Fluids* **2007**, *40*, 74–83. [CrossRef]
148. Ashraful, A.M.; da Silva, G. A detailed chemical kinetic model for the supercritical water oxidation of methylamine: The importance of imine formation. *Int. J. Chem. Kinet.* **2020**. [CrossRef]
149. Makino, M.; Kamiya, M.; Matsushita, H. Computer-assisted prediction of gas chromatographic retention times of polychlorinated biphenyls by use of quantum chemical molecular properties. *Chemosphere* **1992**, *25*, 1839–1849. [CrossRef]
150. Savage, P.E.; Martino, C.; Brock, E.; Mizan, T. Reaction Models For Supercritical Water Oxidation Processes. *Rev. High Press. Sci. Technol.* **1998**, *7*, 1371–1374. [CrossRef]
151. Zhang, J.; Gu, J.; Han, Y.; Li, W.; Gan, Z.; Gu, J. Supercritical Water Oxidation vs Supercritical Water Gasification: Which Process Is Better for Explosive Wastewater Treatment? *Ind. Eng. Chem. Res.* **2015**, *54*, 1251–1260. [CrossRef]
152. *Material Studio*; Accelrys: San Diego, CA, USA, 2001.
153. Parr, R.G.; Yang, W.T. Density functional-approach to the frontier-electron theory of chemical-reactivity. *J. Am. Chem. Soc.* **1984**, *106*, 4049–4050. [CrossRef]
154. Liu, S.B. Conceptual Density Functional Theory and Some Recent Developments. *Acta Phys. Chim. Sin.* **2009**, *25*, 590–600. [CrossRef]
155. Mohamed, I.P.K.; Subramani, K. Structure-Property Analysis of L-Ornithine and Its Substituted Analogues. *Acta Phys. Chim. Sin.* **2009**, *25*, 2357–2365. [CrossRef]
156. Fu, R.; Lu, T.; Chen, F.W. Comparing Methods for Predicting the Reactive Site of Electrophilic Substitution. *Acta Phys. Chim. Sin.* **2014**, *30*, 628–639. [CrossRef]
157. Yang, B.; Cheng, Z.; Yuan, T.; Shen, Z. Catalytic oxidation of various aromatic compounds in supercritical water: Experimental and DFT study. *J. Taiwan Inst. Chem. Eng.* **2019**, *100*, 47–55. [CrossRef]
158. Tan, Y.; Shen, Z.; Guo, W.; Ouyang, C.; Jia, J.; Jiang, W.; Zhou, H. Temperature sensitivity of organic compound destruction in SCWO process. *J. Environ. Sci.* **2014**, *26*, 512–518. [CrossRef]

159. Cheng, Z.W.; Yang, B.W.; Chen, Q.C.; Gao, X.P.; Tan, Y.J.; Yuan, T.; Shen, Z.M. Quantitative-Structure-Activity-Relationship (QSAR) models for the reaction rate and temperature of nitrogenous organic compounds in supercritical water oxidation (SCWO). *Chem. Eng. J.* **2018**, *354*, 12–20. [CrossRef]
160. Ploeger, J.M.; Bielenberg, P.A.; Dinaro-Blanchard, J.L.; Lachance, R.P.; Taylor, J.D.; Green, W.H.; Tester, J.W. Modeling oxidation and hydrolysis reactions in supercritical water—Free radical elementary reaction networks and their applications. *Combust. Sci. Technol.* **2006**, *178*, 363–398. [CrossRef]
161. Webley, P.A. Fundamental Oxidation Kinetics of Simple Compounds in Supercritical Water. Ph.D. Thesis, Massachusetts Institute of Technology, Cambridge, MA, USA, 1990.
162. Zhang, J.; Ma, C.; Sun, Y.; Ren, X.J.R.o.C.I. Hydroxyl radical reactions with 2-chlorophenol as a model for oxidation in supercritical water. *Res. Chem. Intermed.* **2014**, *40*, 973–990. [CrossRef]
163. Zhang, J.; Gu, J.; Han, Y.; Li, W.; Gan, Z.; Gu, J. Analysis of degradation mechanism of disperse orange 25 in supercritical water oxidation using molecular dynamic simulations based on the reactive force field. *J. Mol. Model.* **2015**, *21*, 54. [CrossRef] [PubMed]
164. Jiang, D.; Wang, Y.; Zhang, M.; Zhang, J.; Li, W.; Han, Y. H2 and CO production through coking wastewater in supercritical water condition: ReaxFF reactive molecular dynamics simulation. *Int. J. Hydrog. Energy* **2017**, *42*, 9667–9678. [CrossRef]
165. Ma, T.; Hu, T.; Jiang, D.; Zhang, J.; Li, W.; Han, Y.; Örmeci, B. Treatment of penicillin with supercritical water oxidation: Experimental study of combined ReaxFF molecular dynamics. *Korean J. Chem. Eng.* **2018**, *35*, 900–908. [CrossRef]
166. Ma, J.; Dong, X.; Yu, Y.; Zheng, B.; Zhang, M. The effects of alkalis on the dechlorination of o-chlorophenol in supercritical water: Molecular dynamics simulation and experiment. *Chem. Eng. J.* **2014**, *241*, 268–272. [CrossRef]
167. Alasiri, H. A Molecular Dynamics Simulation Probe of the Solubility Parameters of Supercritical Water and Methanol. *Arab. J. Sci. Eng.* **2019**, *44*, 9911–9917. [CrossRef]
168. Savage, P.E.; Yu, J.L.; Stylski, N.; Brock, E.E. Kinetics and mechanism of methane oxidation in supercritical water. *J. Supercrit. Fluids* **1998**, *12*, 141–153. [CrossRef]
169. Zhang, J.L.; He, Z.H.; Han, Y.; Li, W.; Wu, J.J.X.; Gan, Z.X.; Gu, J.J. Nucleation and Growth of Na2CO3 Clusters in Supercritical Water Using Molecular Dynamics Simulation. *Acta Phys. Chim. Sin.* **2012**, *28*, 1691–1700. [CrossRef]
170. Gong, Y.; Guo, Y.; Sheehan, J.D.; Chen, Z.; Wang, S. Oxidative degradation of landfill leachate by catalysis of CeMnOx/TiO_2 in supercritical water: Mechanism and kinetic study. *Chem. Eng. J.* **2018**, *331*, 578–586. [CrossRef]
171. Dong, X.; Zhang, Y.n.; Xu, Y.; Zhang, M. Catalytic mechanism study on manganese oxide in the catalytic supercritical water oxidation of nitrobenzene. *RSC Adv.* **2015**, *5*, 47488–47497. [CrossRef]